Messinian evaporite deposition during sea level rise in the Gulf of Lions (Western Mediterranean)

François Bache, Julien Gargani, Jean-Pierre Suc, Christian Gorini, Marina Rabineau, Speranta-Maria Popescu, Estelle Leroux, Damien Do Couto, Jean-Loup Rubino, Jean-Louis Olivet, et al.

Marine and Petroleum Geology, in press

Messinian evaporite deposition during sea level rise in the Gulf of Lions (Western Mediterranean)

François Bache[1*], Julien Gargani[2], Jean-Pierre Suc[3,4], Christian Gorini[3,4], Marina Rabineau[5], Speranta-Maria Popescu[6], Estelle Leroux[5,7], Damien Do Couto[3,4,8], Gwenaël Jouannic[2,9], Jean-Loup Rubino[10], Jean-Louis Olivet[7], Georges Clauzon[11], Antonio Tadeu Dos Reis[12], Daniel Aslanian[7]

[1] GNS Science, P.O. BOX 30368, Lower Hutt 5040, New Zealand.
[2] Université Paris-Sud, Laboratoire GEOPS , UMR 8148, Orsay, F-91405, France.
[3] Sorbonne Universités, UPMC Univ Paris 06, UMR 7193, Institut des Sciences de la Terre Paris (iSTeP), F-75005, Paris, France.
[4] CNRS, UMR 7193, Institut des Sciences de la Terre Paris (iSTeP), F-75005, Paris, France.
[5]IUEM, Domaines océaniques (UMR 6538), 1 place Nicolas Copernic, 29280 Plouzané, France.
[6] Geo-Biostrat-Data Consulting, 385 route du Mas Rillier, 69140 Rillieux la Pape, France
[7] IFREMER, Géosciences marines, LGG, BP 70, 29280 Plouzané Cedex, France.
[8]TOTAL, 2 place Jean Millier, 92400 La Défense, Paris, France
[9] CETE Est, LRPC, Nancy, France
[10] TOTAL, TG/ISS, CSTJF, Avenue Laribeau, 64018 Pau Cedex, France.
[11] Aix-Marseille Université, CNRS, IRD, CEREGE UM34, 13545, Aix-en-Provence, France (passed away on March, 12, 2013).
[12] Departamento de Oceanografia Geologica/UERJ-Brazil, Rua São Francisco Xavier, 524, 4º Andar, Maracaña, Rio de Janeiro RJ CEP: 20.550-900, Brazil.

[*] Now at: Santos Ltd, 60 Flinders Street, Adelaide 5000, Australia. francois.bache@santos.com. Tel.: +61 8 8116 7143.

1. Abstract

The Messinian Salinity Crisis resulted from desiccation of the Mediterranean Sea after its isolation from the Atlantic Ocean at the end of the Miocene. Stratal geometry tied to borehole data in the Gulf of Lions show that the pre-crisis continental shelf has been eroded during a major sea-level fall and that sediments from this erosion have been deposited in the basin. This detrital package is onlapped by high amplitude seismic reflectors overlain by the "Messinian Salt" and the "Upper Evaporites". Towards the shelf, the transition between regressive deposits and overlying onlapping sediments is characterised by a wave-ravinement surface, suggesting that a significant part of the onlapping reflectors and overlying Messinian Evaporites were deposited during a relatively slow landward migration of the shoreline. The clear boundary between the smooth wave-ravinement surface and the subaerial Messinian Erosional Surface observed on the Gulf of Lions shelf and onshore in the Rhône valley is interpreted to have resulted from a rapid acceleration of the Mediterranean sea level rise at the end of the Messinian Salinity Crisis. Numerical simulation of this cycle of sea level change during the Messinian Salinity Crisis and of precipitation of thick evaporites during the slow sea level rise shows that this scenario can be modelled assuming a value of evaporation minus precipitation of 1.75 $m^3/m^2/yr$ in the deep Mediterranean basins.

Keywords: Messinian; Mediterranean; Gulf of Lions; Seismic stratigraphy; Evaporites.

2. Introduction

The largest known sea level fall on the Earth resulted from the isolation of the Mediterranean Sea from the Atlantic Ocean at the end of the Miocene. This isolation, associated with a significant evaporation rate, led to the deposition of a series of thick evaporites in the Mediterranean basins (Hsü et al., 1973a) and intense subaerial erosion at its periphery (Barber, 1981; Barr and Walker, 1973; Chumakov, 1973; Clauzon, 1973, 1978, 1982; Ryan and Cita, 1978; Savoye and Piper, 1991). The "desiccated, deep basin" model (Hsü, 1972b; Cita, 1973; Hsü et al., 1973a; Ryan, 1973) explains this depositional event, known as the Messinian Salinity Crisis (MSC), by a high evaporation rate and sea-level drop of around 1500 m in a deep Mediterranean basin[1] (Cita, 1973; Hsü, 1973; Hsü et al., 1973b; Hsü and Bernoulli, 1978; Montadert et al., 1978; Stampfli and Höcker, 1989). Three arguments have been used to strengthen this theory: the tidal nature of the evaporites recovered in all the major basins (Hsü, 1972a, b); the pan-Mediterranean distribution of seismic reflector M that was calibrated with the abrupt contact between the evaporites and the overlying Early Pliocene marls (Ryan, 1973), and the open marine, deep bathyal nature of the pelagic sediments immediately superposed on the evaporites (Cita, 1973). This argument was also supported from studies on products of the marginal erosion coeval with the deep basin evaporites all around the Mediterranean (Barr and Walker, 1973; Chumakov, 1973; Clauzon, 1973, 1974; Cita and Ryan, 1978; Clauzon, 1978; Rizzini et al., 1978; Ryan and Cita, 1978; Clauzon, 1979; Barber, 1981; Clauzon, 1982). In the 1990s, the peripheral Mediterranean basins accessible to field studies were used to constrain the timing of the MSC (Hilgen and Langereis, 1993; Gautier et al., 1994; Krijgsman et al., 1999a; Van Couvering et al., 2000; Lourens et al., 2004). No physical link has been established between these basins and offshore Mediterranean deep basins and evaporites from the deep basins have not been fully sampled or accurately dated. Therefore the timing and the environment of evaporites deposition in the Mediterranean deep basins is still uncertain and controversial.

Two groups of conceptual scenarios are usually referred to (Fig. 1): one that favours a synchronous deposition (at 5.96 Ma) of the first evaporites in all the Mediterranean basins before the huge sea level fall (Krijgsman et al., 1999a; Rouchy and Caruso, 2006), and the second that favours a diachronous deposition of the evaporites through two phases of desiccation (Butler et al., 1995; Clauzon et al., 1996; CIESM, 2008). According to the second scenario, peripheral basins experienced deposition of evaporites from 5.971 Ma (Manzi et al., 2013) to 5.600 Ma after an initial sea level fall (~150 m, phase 1): in this paper, we call these the "1st step evaporites". Then, from 5.600 to 5.460 Ma (Bache et al., 2012) the Mediterranean deep basins experienced a major sea-level fall (1500 m) and deposition of evaporites in almost completely desiccated environments. In this paper we call them the "2nd step evaporites". During this second phase (the "peak of the MSC"), the "1st step evaporites" were partly eroded and reworked.

Interpretation of the environmental setting of some basins is also controversial. For example, the Sicilian Caltanissetta Basin has been interpreted as either a deep basin that was subsequently uplifted (Hsü et al., 1973a; Krijgsman et al., 1999a; Rouchy and Caruso, 2006; Roveri and Manzi, 2006; Krijgsman and Meijer, 2008), containing only "2nd step evaporites", or as a peripheral basin (Brolsma, 1975; Butler et al., 1995; Clauzon et al., 1996; Popescu et al., 2009) containing the "1st step evaporites". Following the former interpretation, Roveri and

[1] According to their geographic respective location, we distinguish (1) peripheral basins characterised by continuous shallow-water conditions in the Messinian and Zanclean (most of them being onshore today), and (2) deep basins where deep marine conditions prevailed except during the peak of the MSC.

Manzi (2006) questioned the existence of a significant (>1000 m) Messinian sea level drawdown and argued in favour of widespread tectonic movements to explain observations all around the Mediterranean. On the other hand Roveri et al. (2008a; 2008b) opted for the occurrence of the two steps of evaporites in Sicily which includes peripheral basins (Calatafimi-Ciminna, Belice, Licodia) and an intermediate basin (Caltanissetta).
In order to clarify the events that affected the Mediterranean basins, we describe the marginal transition from the Gulf of Lions shelf to the Provence deep Basin. Stratal relationships between the subaerial erosional surface, clastic deposits generated by this erosion and evaporites allow us to discuss the mode of deposition of the "2nd step evaporites" and to test a refined scenario with a numerical model.

3. Data and method

The Gulf of Lions (Fig. 2) is weakly deformed by Pliocene and Quaternary tectonics and characterised by a relatively high subsidence rate which continuously created accommodation space (Steckler and Watts, 1980; Bessis, 1986; Burrus, 1989; Rabineau et al., 2005; Bache et al., 2010). This configuration, together with the availability of a large set of seismic reflection data (Fig. 2), has allowed accurate descriptions of the relationship between the Messinian halite and the sedimentary units of the Gulf of Lions margin (Gorini, 1993; Lofi et al., 2005; Bache, 2008; Bache et al., 2009). In this study, conventional and high-resolution seismic reflection data are reviewed and interpreted using the principles of seismic stratigraphy (Vail et al., 1977). The extensive coverage of seismic data enabled an integrated seismic stratigraphy to be developed, with seismic unit identification based on the configuration of seismic reflectors, including reflector continuity and termination. Interpretation and correlation of seismic reflectors has been tied to biostratigraphic and lithostratigraphic data from eleven hydrocarbon exploration wells that sampled Miocene and younger sedimentary cover. Seismic two-way travel-time (TWT) has generally been tied to formation tops in wells using velocities from sonic logs. Data used for this study and time-depth relationships are summarised in Supplementary Figures 1 and 2.
We also used observations from dive 72 from the submersible *Cyana* (with Syledis positioning) during cruise MONICYA in 1989 on the *Suroit* vessel. Dive 72 was carried out along the western slope of the Cirque Marcel, where the Quaternary submarine erosion exposes a section through older rocks (Savoye and Piper, 1991: fig. 9). Here we present new complementary observations to those already published by Savoye and Piper (1991).
Finally a "water-budget" numerical model is used to test if our scenario of the MSC is reliable under realistic hydro-climatic conditions. The modelling method has been developed in several studies (Blanc, 2000; Meijer and Krijgsman, 2005; Blanc, 2006; Meijer, 2006; Gargani and Rigollet, 2007; Gargani et al., 2008) and details are also reported in the "numerical model" section. Atlantic sea water inflow, river discharge and rainfall are taken into account with our observations and counterbalanced by the rate of water evaporation. The evaporation minus precipitation (E-P) value used in the model to produce results compatible with our observations and interpretations is discussed and compared with present day values.

4. Review of previous observations

Here, we review existing observations and interpretations related to the MSC in the Gulf of Lions. We use a new, non-interpretative, naming convention for seismic units and unconformities, which can be compared to existing nomenclature in Supplementary Figure 3.
Six seismic units (named U1 to U6 in this study) bounded by unconformities (S1 to S4) can be differentiated (Fig. 3). S2, a major unconformity at the transition between synrift and postrift deposits (Guennoc et al., 2000; Bache et al., 2010), marks the lower boundary of this study.

Seismic unit U3 overlies S2 and is characterised by parallel and continuous reflectors that prograde with an offlap break located approximately below the present-day slope (Figs. 3 and 4). U3 is commonly considered as a wide Aquitanian to Tortonian prograding shelf based on seismic interpretations (Guennoc et al., 2000; Bache et al., 2010) and benthic and planktonic foraminifers found at wells (Fig.5) (Cravatte et al., 1974; Guennoc et al., 2000). U3 is locally deformed in the western part of the Gulf of Lions where faults and roll-over tilting are observed (Mauffret et al., 2001; Gorini et al., 2005; Lofi et al., 2005). U3 is regionally truncated by two distinct unconformities, S3 and S4 (Figs. 3 and 4).

Unconformity S3 is inclined (~2.5°) toward the basin and has been mapped in detail with high resolution and conventional seismic reflection data (Lofi and Berné, 2008; Bache et al., 2009). The surface truncates the prograding reflectors of U3 and is made of two major incisions (up to 1500 m) filled by seismic unit U4 (Figs. 2, 6 and 7).

Seismic unit U4 is composed of 3 sub-units separated by minor unconformities (see Bache et al., 2009 and Lofi and Berné, 2008). U4a and U4b are characterised by clinoforms that dip steeply basinward and extend beneath U5 (Figs. 8 and 9). U4a is between 2424 and 2997 m in Autan 1 and described as undetermined Middle to Upper Miocene calcareous shale (Fig.5; Cravatte et al., 1974). U4b is between 3703 and 4650 m in well GLP 2 and described as Middle to Upper? Miocene (Langhian to Tortonian) calcareous shale (Figs.5 and 10; Brun et al., 1984). U4c is characterised by a chaotic high-amplitude seismic facies passing laterally to the upper part of U5 (Lofi et al., 2005; Lofi et al., 2011) and has never been drilled.

Despite the sampling of U4a and U4b by Autan 1 and GLP 2 wells (Figs. 5, 6, 10 and 11), two conflicting interpretations for their age and for the age of their basal unconformity S3 have been proposed. One interpretation gives an age between 16.4 Ma and 5.6 Ma for the deposition of U4a and U4b, i.e. before the peak of the MSC (Lofi and Berné, 2008). The other interpretation links S3, U4a and U4b with the main MSC sea level fall at 5.6 Ma (Bache et al., 2009). U4c is classically interpreted as resulting from margin erosion during the peak of the MSC (Lofi et al., 2005; Lofi and Berné, 2008; Bache et al., 2009). Interpretations of S3, U4a and U4b and consequences for the MSC will be developed in the "Refining our scenario for the peak of the MSC" section.

S4 is characterised by two distinct morphologies. S4rough is a rough surface that truncates U3 on the shelf (Ryan and Cita, 1978; Gennesseaux and Lefebvre, 1980; Lefebvre, 1980; Gorini, 1993; Guennoc et al., 2000; Lofi et al., 2005; Bache et al., 2009). Mapping reveals a pattern of up to 5th order dendritic drainage with two main systems (Fig. 2) (Gennesseaux and Lefebvre, 1980; Guennoc et al., 2000; Lofi et al., 2005; Bache et al., 2009). The two systems have been mapped upstream in the Languedoc-Roussillon region and in the Rhône Valley where erosion is observed up to at least 350 km from the present coast (Clauzon, 1978, 1979, 1982a). Boreholes Tramontane 1, Calmar 1 and Mistral 1 show that S4rough truncates Upper Miocene sediments (U3) and is covered by sediments of the earliest stage of the Pliocene (U6) (Fig.5) (Cravatte et al., 1974; Guennoc et al., 2000). S4rough is commonly interpreted as a subaerial erosional surface (the Messinian Erosional Surface or Margin Erosion Surface, MES) sculpted during the main MSC sea level fall (Ryan and Cita, 1978; Guennoc et al., 2000; Lofi et al., 2005; Bache et al., 2009). S4rough gives way basinward to a planar and smooth morphology (S4smooth) that is locally conformable with U3 but that is also locally erosional as it truncates U4 (Figs. 3 and 6 to 8). The transition between S4rough and S4smooth lies at a constant two-way traveltime depth of 1.6 seconds over most of the shelf (Bache et al., 2009; Bache et al., 2012). This difference of morphology has been explained either by retrogressive erosion during a MSC relative sea level fall (Lofi et al., 2005) or by a two-step reflooding process ending the MSC (Bache et al., 2012). In this later interpretation, S4smooth represents a transgressive ravinement surface created during a first step of reflooding and S4rough represents a subaerial surface (i.e. the MES) preserved from wave

erosion after a sudden acceleration of the reflooding (rapid enough to prevent wave abrasion). The preserved shoreline at the point where S4smooth (wave cut surface) meets the S4rough (subaerial erosion) is thought to represent the shoreline or a zero sea level marker just before the final rapid reflooding (Bache et al., 2012).

Seismic unit U5 is composed of 3 sub-units (U5a, U5b and U5c). U5a is a 1500 m thick unit characterised by continuous parallel high-amplitude reflectors (Figs. 3, 8 and 12) (Bache et al., 2009). The lower part of U5a shows onlap terminations on U4b (Figs. 3, 8 and 12, see also Supplementary Figure 6). Its upper part has been described as a lateral equivalent of the chaotic sub-unit U4c (Lofi et al., 2005). U5b is a transparent seismic facies characterised by domes structures and U5c is made of a group of parallel and relatively continuous reflectors that onlap landward onto the top of U4 (Figs. 3 and 8). U5a (or its upper part), U5b and U5c have classically been interpreted as the three components of the "2nd step Evaporites" (Lower Evaporites, Salt, Upper Evaporites) of the MSC in the Mediterranean deep basins (Lofi et al., 2005; Bache et al., 2009). The "massive salt" (U5b) is the most common facies of the Messinian in the Gulf of Lions deep basin. Domes were formed after the Early Pliocene and during the deposition of the Pliocene and Quaternary turbidites (Dos Reis et al., 2005). The "Upper Evaporites" (U5c) is the only member of the trilogy that has been drilled (Hsü et al., 1973b). It is made-up of intercalated beds of anhydrite and clay (Ryan et al., 1973) and has been deformed by creeping and sliding of the underlying salt and by listric faulting (Dos Reis et al., 2005). Either the upper part of U5a (Montadert et al., 1978; Lofi et al., 2005) or the entire sub-unit (Bache et al., 2009) have been interpreted as the "Lower Evaporites" (probably intercalated with detritus from the margin erosion) but have never been drilled so that their lithology is still unknown.

Seismic unit U6 is observed in the entire region and lies above U3, U4 or U5 (Figs. 3 and 8). This unit, running from Lower Pliocene to Quaternary (Fig. 5, Cravatte et al., 1974), shows prograding sediments downlapping directly onto S4rough is interpreted as an overall regressive sequence characterised by the reconstruction of shelf-slope geometries (Lofi et al., 2003; Rabineau et al., 2005). The basal geometric configuration of U6 (downlaps on S4rough and absence of transgressive deposits) has been interpreted as the consequence of a very rapid reflooding at the end of the MSC (Lofi et al., 2003; Lofi et al., 2005). This rapid reflooding is also suggested by a sharp contact between the Messinian "2nd step evaporites" and Zanclean mudrocks drilled in the Western Mediterranean Basin during DSDP expeditions (Cita et al., 1978). Onshore, this contact corresponds to the prograding sedimentary filling of widely distributed Gilbert-type fan deltas within the Zanclean rias without any onlapping transgressive parasequence (Clauzon, 1990).

5. New observations

We provide new key observations and detail stratal relationship between U3, U4 and U5, together with a critical review of well data information. These observations are critical for interpreting the mode of deposition of the Messinian evaporites.

5.1. *Transition between U3 and U4 (S3)*

Previous analyses of borehole data concluded an Aquitanian to Tortonian age for U3 (Tramontane 1, Mistral 1, Calmar 1) and a Langhian to Tortonian age for U4 (GLP 2, Autan 1), suggesting that part of these units may have been deposited contemporaneously (Fig. 5). However, the presence of a major unconformity between the two seismic units (S3) indicates that U4 is younger than U3 (Figs. 6 and 7).

U3 is made of parallel and continuous strata easy to follow and correlate on seismic data, all wells give a general agreement on its Miocene age and marine depositional environment. No major hiatuses or erosion can be observed on the seismic data and strata show a general agradationnal stacking pattern with no evidence of reworking (Figs. 3 and 4). Seismic

horizons within U3 therefore provide characteristic age markers that can be used to constrain the age of U4. We have interpreted five horizons within U3 (H1 to H5 on figures) that are tied to boreholes (Figs. 3 to 6). All these horizons can be followed towards the basin below S4; H1 to H5 are therefore older than U4. We can then assume that the age of the shallowest horizon (H5) also corresponds to the maximum age for U4 deposition.

H5 intersects three wells at the exact position of a clear change in depositional environment corresponding to a regression (from slope or shelf to littoral facies in Mistral 1) or just above it (in Tramontane 1 and Calmar 1 boreholes) (Fig. 5). In Tramontane 1 and Mistral 1 boreholes the change, respectively located at 1540 and 1675 m depth, also corresponds to a clear regression with a transition from marine to littoral conditions (Fig. 5; Cravatte et al., 1974). The littoral sediments are dated from Middle (Langhian-Serravallian) to Upper Miocene (Tortonian-Messinien) (Fig.5, Cravatte et al., 1974). In Calmar 1, the contact is located at 1420 m and has been ascribed to the Serravallian/Tortonian transition, i.e. around 11 Ma (Fig. 5; Guennoc et al., 2000). This age (which is the most precise) therefore suggests that deposition of U4 occurred after 11 Ma. As U4 is also overlain by U6 (earliest Pliocene to Quaternary), we conclude that this unit has been deposited later than 11 Ma and before the end of the MSC, usually placed at 5.332 Ma (Hilgen and Langereis, 1993; Van Couvering et al., 2000; Lourens et al., 2004) but recently revised at 5.460 Ma (Bache et al., 2012). Note also that erosion reaching more than 1000 m was observed on the shelf above this H5 horizon (Lofi et al. 2005; Bache et al., 2009).

Age inconsistency for U4 in GLP 2 and Autan 1 boreholes may be explained by reworking. The seismic facies observed in U4 clearly show evidences of reworking with strong erosion observed at its base and internal truncation and erosional surfaces. Some indications of reworking were also found within U4 in GLP 2 (Brun et al., 1984) suggesting that U3 fauna may have been reworked within U4 during a significant sea level fall (Bache et al., 2009). Micropaleontologic assemblages are also generally poor in stratigraphic markers in GLP 2 (Brun et al., 1984).

5.2. *Transition between U4 and U5*

In GLP2, a heterogenous evaporitic body (166 m thick) has been sampled between 3437 and 3603 m depth that comprises alternate layers of halite, clays and anhydrite (Figs. 10 and 11). Fifty two metres of sandstones (between 3385 m and 3437 m) overlie the evaporites and contain a clay layer at 3426.70 m depth with a calcareous nannoflora containing *Amaurolithus primus* and *A. tricorniculatus* (Fig. 11, Brun et al., 1984) that in the absence of *Discoaster quinqueramus* and *Ceratolithus acutus* can be dated between 5.54 and 5.35 Ma (Raffi et al., 2006; Di Stefano and Sturiale, 2010). This indicates a late Messinian age for the evaporitic body, which is also supported by the presence of *Globigerina nepenthes* at 3508.70 m depth (Brun et al., 1984).

The evaporitic unit sampled in GLP 2 extends toward the basin within the upper part of U5a (Fig. 9). U5a is characterised by a general retrogradational pattern with onlap terminations on U4 and S4smooth (Figs.8, 9 and 12, see also Supplementary Figure 6). It means that a significant part of U5 (upper part of U5a, U5b and U5c) has been deposited during or after the formation of S4smooth. This observation contrasts with previous interpretations assuming that only the "Upper Evaporites" (U5c) and the 52 m of sandstones drilled in GLP 2 were deposited during a transgressive phase that shaped S4smooth (Bache et al., 2009; Bache et al., 2012).

5.3. *Complementary dive observations*

The region offshore the French Riviera is suitable for dive observations because of the Quaternary cutting of sub-marine canyons that exposes deposits along a large present-day bathymetric range. In this area, a detritic fan and "2nd step evaporites" have been mapped by Savoye and Piper (1991) according to seismic profiles (Fig. 13A) but these authors did not

clearly show the relationship between the detrital deposits and these evaporites. The detritic fan is exposed in the Cirque Marcel (Fig. 13A) where cross bedded sandstones at 2152 m below sea level (bsl) (Fig. 13B) have been described below conglomerates (from *ca*. 2100 to *ca*. 2000 m bsl) (Fig. 13C) and marls (above 1950 m bsl) (Fig. 13D) (see also Savoye and Piper, 1991: fig. 13).
An unpublished photograph of the conglomerates show that they comprise rounded pebbles cemented by a reddish matrix (Fig. 13B). Rocks with similar colour are not known in the drainage basin landward of the Nice – Monaco area and suggests that these conglomerates may have been exposed to weathering processes. As these deposits are immediately overlain by bedded silty turbidites (Fig. 13D) dated from the early Zanclean (Savoye and Piper, 1991), we propose to ascribe the conglomerates to the Messinian lowstand detritic fan. However, alternative age interpretations may exist. Similar land-deposited conglomerates characterize in the region the beginning of the continental syn-rift Oligocene deposits, forced by intensive tectonics and erosion, such as the Vazzio and Ussana formations in southwestern Corsica (Ferrandini et al., 1999) and southern Sardinia (Cherchi et al., 2008), respectively. There, alluvial fans are narrowly linked to proximity of a high relief. Such a Corsican important relief is considered to have provided the pollen grains of altitudinal trees recorded in the early Aquitanian clays of the Vence Basin near Nice (Suc et al., 1992; Fauquette et al., accepted), consistently with palaeogeographic reconstructions (Meulenlamp and Sissingh, 2003; Cherchi et al., 2008). But Savoye and Piper (1991) have undoubtedly shown the north origin of the conglomerates evidenced by the dives whereas the absence of important relief northward the Nice area is established at the earliest Miocene (Fauquette et al., accepted, and references herein). In a subsidence – uplift reconstruction, Savoye and Piper (1991) evidenced that this subaerial detritic fan deposited at an altitude of about 1100-1300 m below the present-day sea level, a value inconsistent with the Oligocene sea level fall (Haq et al., 1987; Miller et al., 2001) but consistent with the Messinian sea level drop of the Mediterranean. For the above-mentioned reasons, an Oligocene age cannot be considered for the palaeo-Var conglomerates. According to Savoye and Piper (1991), this detritic fan is "restricted to channels on the Messinian surface". Taking also into account the early Zanclean age of the overlying turbiditic marls indicated by foraminifers, they suggested that deposition of these conglomerates followed the post-MSC marine reflooding. However, it has been recently established that this detritic fan was stopped inland at that time of high sea level, being illustrated by the Carros breccia (Bache et al., 2012). We thus conclude that deposition of this detritic fan just before the 2nd step Messinian evaporites remains the most suitable hypothesis.
At last, according to J.-P. Réhault (*in litteris*, 2012), such fluvial conglomerates with a matrix suggesting rubefaction have been commonly observed in several dives in the area, asserting that the major detritic fans are, in the basin, re-covered by the Messinian halite (2nd step evaporites) despite some lateral shifts.

6. Refining our scenario for the peak of the MSC

6.1. *Deposition of U4 during the main Messinian sea-level fall*

We have constrained the age of deposition of U4 between 11 Ma and the end of the MSC. Existing interpretations for the age of deposition of U4a and U4b, i.e. before or during the MSC, can thus be discussed with respect to this time interval.
Lofi and Berné (2008) interpreted erosion of S3 at the base of U4a and U4b to one, or the combination of several factors among which (1) the occurrence of fluctuations in sea level after 16.4 Ma (especially the pronounced sea-level fall that occurred at the Serravallian/Tortonian transition) and (2) a local tectonic event on the western platform of the Gulf of Lions. These authors disregard the deposition of U4a and U4b during the MSC because (1) the identification of five successive generations of submarine canyons at the base

and within U4a and U4b and (2) aggradational geometry of the topsets beds observed within one of the interpreted canyons that seems incompatible with a major MSC lowering phase. However, our observations from seismic and wells show that the Serravallian/Tortonian transition (reflector H5) extends below S3 (Fig. 6). The corresponding pronounced sea-level fall cannot therefore be responsible for S3 erosion and the deposition of U4a and U4b.

The western part of the Gulf of Lions is characterised by the presence of normal faults that have affected U3 before the S4rough event (Fig. 3). This configuration highlights the existence of a local Upper Miocene tectonic event (Mauffret et al., 2001; Gorini et al., 2005; Lofi et al., 2005). Lofi *et al.* (2008) suggested that this episode, probably accompanied by an increase of clastic sediment supply, is a possible origin for the formation of S3 and subsequent filling with U4a and U4b. In order to decipher the tectonic and eustatic origin of theses canyons, the same authors suggest looking for the existence of sub-marine canyons in the eastern Gulf of Lions, an area where the Upper Miocene tectonics has not been observed. The recent identification of U4a and U4b prisms and their basal major incision (S3) in the eastern part of the Gulf of Lions (Figs. 2 and 4; see also Bache et al, 2009) therefore suggests that the tectonic hypothesis alone cannot explain the sedimentary geometries in the Gulf of Lions.

Bache et al. (2009) interpreted U4a and U4b prisms as the detrital sediments reworked by S4rough erosion. This interpretation is supported by the quantitative assessment of eroded and deposited volumes (Lofi et al., 2005; Bache et al., 2009) which shows that the volume of the entire U4 unit (9400 km^3) is similar to the estimated volume of eroded material (more than 10000 km^3). Bache et al. (2009) also argued that the most prominent erosional event (i.e. erosion of the margin during the peak of the MSC) must have been recorded seaward by the most prominent geological features, i.e. S3 and U4a/U4b prisms.

Our observations show that a direct correlation between S4rough (Messinian erosion) and the entire U4 unit is the only hypothesis that is consistent with our time-window for the deposition of U4. The existence of sub-marine canyons at the base and within U4 (Lofi and Berné, 2008) is not inconsistent with a MSC sea-level drop. These canyons could have been formed at the beginning of the MSC sea-level fall, when the shelf was already exposed to subaerial erosion, but before the end of the regressive phase. We therefore do not exclude the influence of subaqueous processes for the formation of the S3 unconformity, which could correspond to a "basal surface of forced regression" *sensu* Hunt and Tucker (1992). In fact, this is exactly what is observed on the shelf of the Gulf of Lions during Quaternary lowstands with a regressive surface of marine erosion at the base of forced regressive prisms (Rabineau et al., 2005).

6.2. *Transgressive evaporites (U5)*

Drawdown and shrinkage of pre-concentrated brine bodies (Hardie and Lowenstein, 1985) have been argued to explain the distribution of salt across much of the sea floor beyond the shelf edge but inversely proportional in thicknesses to elevation above the basin floor (Ryan, 2009). Halite deposits would therefore be thin on slopes, thicker on deep-sea fan aprons and thickest on the abyssal plains (Ryan, 2009). Such distribution is true for the Gulf of Lions. However, our observations also show that a significant part of U5 (upper part of U5a, U5b and U5c) is deposited with an onlap configuration against S4smooth, which truncates older deposits (U4).

Interpretation of S4smooth as a wave ravinement surface is argued based on its smooth morphology and its geometric relationship with underlying and overlying units (Bache et al., 2009; Bache et al., 2012). One of the most compelling observations that supports this interpretation is the landward transition of S4smooth with S4rough, which can be observed at a constant depth (1.6 s TWT) in the whole Gulf of Lions margin (Bache et al., 2009; Bache et al., 2012). Such a transition, between a deeply incised, typical subaerial surface (S4rough,

MES) and a smooth surface (S4smooth) with erosional truncations below and onlaps above, is likely to represent the paleoshoreline at the end of the wave abrasion.

Erosional truncation implies the deposition of strata and their subsequent removal (Mitchum et al., 1977). Onlap is a relation in which seismic reflections are interpreted as initially horizontal strata terminating progressively against an initially inclined surface, or as initially inclined strata terminating progressively updip against a surface of greater inclination (Mitchum et al., 1977). This stratal relationship between U4 and U5a together with the presence of a wave-ravinement surface (S4smooth) between the two units suggest that a significant part of the "2nd step evaporites" (upper part of U5a, U5b and U5c) was deposited during a landward migration of the shoreline (transgressive trend) that also reshaped previous topography to form S4smooth. This interpretation is also supported by the presence of clays within U5 (sampled in GLP 2) characterised by 80% planktonic foraminifers (at 3508.70 m from a side well core; Fig. 11; Brun et al., 1984), suggesting the occurrence of fully marine conditions in the basin and thus compatible with deposition of U5 during sea-level rise.

Landward migration of the shoreline implies an increase in accommodation that can be caused by (i) subsidence, (ii) a rise of the Mediterranean sea level or (iii) a combination of both. Transport of sediment from the eroded margins to the basin, accompanied by a high precipitation rate of evaporites, can generate subsidence in the deep basins by loading. However observation of a smooth surface comparable to S4 smooth almost exactly at the same depth (1.4-1.7 s TWT) in the Valencia Trough (García et al., 2011) suggests the influence of a Mediterranean sea-level rise. Submarine terraces have also been described in the Alboran margin (Estrada et al., 2011) and SW Mallorca Island and Bay of Oran (Just et al., 2011), and could be a consequence of this potential sea-level rise. This transgressive context coupled with a high evaporation rate provided favourable conditions for the precipitation of thick "2nd step evaporites".

The large amount of salt precipitated during the MSC requires the evaporation of about 8 times the volume of the present-day Mediterranean and thus implies continuous seawater input to the Mediterranean during the precipitation stage (Hsü et al., 1977; Benson et al., 1991; Blanc, 2006; Gargani et al., 2008; Ryan, 2009). Recent numerical models suggest that such input is insufficient or unlikely to occur after the closure of the Rifian Corridor (Blanc, 2002; Garcia-Castellanos et al., 2009; Govers, 2009; Govers et al., 2009), the age of which is well-constrained at 5.60 Ma at its Mediterranean and Atlantic exits (Krijgsman et al., 1999b; Warny et al., 2003). Precipitation in all the basins before any significant Messinian sea-level fall and before the total isolation of the Mediterranean (Krijgsman et al., 1999a) has been reproduced with numerical models (Meijer and Krijgsman, 2005; Blanc, 2006; Ryan, 2008; Garcia-Castellanos and Villasenor, 2011). However sedimentary geometries in the Gulf of Lions do not support this hypothesis, which would imply major erosion and detritic deposition after the deposition of thick "2nd step evaporites". Our observations rather show major erosion (S3 and S4rough) and detrital sediment deposition (U4) before evaporite precipitation (U5). Loget et al. (2005) have shown that intense regressive erosion developed in the Gibraltar area after the Messinian sea-level drawdown. This process could result from a continuous input of ocean water to precipitate enough evaporites in an almost completely desiccated Mediterranean Basin.

Hardie and Lowenstein (2004) re-interpreted cores from DSDP Legs 13 and 42A and suggest that (upper) evaporites of the Mediterranean deep basins were deposited under "relatively deep-water (below wave base) conditions". Considering that only a small part of the upper stratigraphic units of the evaporitic body have been sampled (tens of metres), these authors noted that "*Until we have deep cores that penetrate the entire evaporite section we cannot hope to unravel more from existing DSDP cores than the depositional history of the very last phase of the Messinian evaporite body that lies beneath the floor of the Mediterranean Sea*".

Deep-water (below wave base) conditions for the top of the evaporite unit are in agreement with deposition during sea-level rise.

6.3. *A three-step scenario for the peak of the MSC*

The largely accepted diachronous scenario of Messinian evaporites (Clauzon et al., 1996; CIESM, 2008) involves the isolation of "peripheral" basins and "1st step evaporites" deposition with an initial sea-level fall followed by deposition of "2nd step evaporites" in the deepest parts of the Mediterranean after a major drawdown. A relative fall and rise of the Mediterranean sea level at the end of the Miocene is commonly proposed to explain observations in the Gulf of Lions (Guennoc et al., 2000; Gorini et al., 2005; Lofi et al., 2005; Bache et al., 2009). This interpretation is supported by the observation of conglomerates with reddish matrix resulting from oxidation in the Cirque Marcel. Indeed, the present depth of this Messinian fluvial conglomerates at more than 2000 m bsl (a depth somewhat increased by Pliocene subsidence) is consistent with a significant sea level fall during the Messinian.

Our new observations in the Gulf of Lions also support this scenario. Seismic unit U4 has been deposited during the desiccation phase (2-I) and a significant part of U5 ("2nd step evaporites") has been deposited during a relatively slow transgressive phase (2-II), just before the final rapid re-flooding (2-III) (Figs. 14 to 16). This three-step scenario for the peak of the MSC is a simplification of the four-step scenario of Bache et al. (2009) where the deposition of the "2nd step evaporites" and the relatively slow transgressive phase were separated into two different steps. This new scenario should provide a solution to the controversy about water depth over the "2nd step evaporites" during their deposition.

Similarities of seismic records between the Western and Eastern Mediterranean basins have been shown and discussed by Bache et al. (2012). Indeed, in the Eastern Mediterranean, the "2nd step evaporites" are sandwiched between thick clastic deposits (Bertoni and Cartwright, 2007; Montadert et al., 2011) and an abrasion surface located just below the earliest Pliocene sediments (Bertoni and Cartwright, 2007). These observations, comparable to observations in the Western Mediterranean, could be explained by similar sea level variations in the two Mediterranean basins assuming a relatively low sill between Sicily and Tunisia. On the contrary, a marine water input from the Red Sea is to be foreseen.

7. Numerical model

7.1. *Model setup*

To obtain the interpreted sea level variation and to predict the observed evaporite thickness in the Western Mediterranean Basin, it is necessary to calculate the water budget and to take into account the geometry of the basin. Instead of using a semi-empirical equation to simulate the erosion of the Gibraltar sill and the theoretical increase of the Atlantic flux $Q_{ocean}(t)$, we estimate the best set of Atlantic flux $Q_{ocean}(t)$ and E-P that allow the model to fit our observations (sea-level variation, timing and evaporite thickness). This approach allow us to verify the global coherency of the proposed scenario and to estimate a first order quantitative value for several parameters (E-P and $Q_{ocean}(t)$) that permit to obtain a realistic simulation. The water budget of the Western Mediterranean Basin is estimated by summing the discharge from rivers $Q_{river}(t)$, the precipitation $P(t)$ and the Atlantic Ocean flux $Q_{ocean}(t)$. The fresh water loss by evaporation $E(t)$ is also taken into account. For simplification, $Q_{river}(t)$, $P(t)$ and $E(t)$ are considered constant during the simulation. $Q_{ocean}(t)$ is not constant and increase with time. This increase is calibrated to allow the model to fit the sea level variations and the evaporate thickness observed. Starting from an initial volume of sea water V_0 of the Western Mediterranean Basin a new volume $V(t+1)$ is calculated at the time t. The water budget is given by:

$$\Delta V(t+1) = V_0 - V(t+1) = V_0 + (Q_{river}(t) + P(t) + Q_{ocean}(t) - E) \cdot S(t) \cdot t$$

Using the water budget calculated $\Delta V(t+1)$, we estimate the Mediterranean Sea surface at the next step using the equation $S^2(t+1) = S^2(t) - 2\Delta V(t+1)/a$. The sea level of the Mediterranean $Z(t+1)$ is calculated from the area of the Mediterranean Sea $S(t+1)$ using the equation $Z(t+1)=a.S(t+1)+Z_0$, where a and Z_0 are parameters that depend on the geometry of the Western Mediterranean Basin at the Messinian time. For the Western Mediterranean Basin a and Z_0 are assumed to be equal to 4461.5×10^{-12} m^{-1} and to -3123 m respectively. During the MSC in the Mediterranean area, the evaporation E was higher than the sum of the water influx triggering a drawdown of the Mediterranean sea level Z(t+1) during part of the crisis until the increase of the Atlantic flux $Q_{ocean}(t)$ allowed the progressive reflooding of the Mediterranean.

To calculate the evaporite thickness, it is necessary to know the water volume V(t) and the salt concentration C(t). The salinity of the Mediterranean Sea at the beginning of the crisis C_0 is considered to be 35 g/l, equal to the salinity of the Atlantic Ocean C_{ocean}. The salinity of rivers C_{river} is assumed to be of 1 g/l. The salt concentration of the Western Mediterranean Basin at time t is therefore given by:

$C(t) = [M_0 + M_{river}(t) + M_{ocean}(t)] / V(t)$

where $V(t)$ is the volume of the sea water at the time t and $M_0 = C_0.V_0$ is the mass of evaporites when all the water in the Western Mediterranean is evaporated.

$M_{river}(t) = Q_{river}(t) . C_{river} . t$ is the mass of evaporites which come from river discharge Q_{river}, $M_{ocean}(t)=Q_{ocean}(t) . C_{ocean} . t$ is the mass of evaporites which come from the Atlantic Ocean through an oceanic inflow $Q_{ocean}(t)$ when Atlantic Ocean waters flooded over the Gibraltar sill. The salt precipitates when $C(t)$ >130 g/l. This precipitation allows the formation of evaporite minerals. The salt density used to calculate the volume of evaporites is 2170 kg/m^3.

7.2. *Model implications*

Input variables (precipitation, evaporation, river discharge, Atlantic sea water inflow) were chosen in order to honour our geological observations and interpretations (Fig. 16) and thus determine if their values are realistic. Model inputs include a 1500 m sea-level drawdown at 5.60 Ma; deposition of the thick "2nd step evaporites" body starting after the sea-level fall and during a slow sea-level rise from -1500 m to -900/-600 m depth (Bache et al., 2012), followed by an instantaneous re-flooding. Our numerical simulation (Fig. 17) shows that (1) the sea level in the deep basins and the thickness of the evaporites are strongly dependent on evaporation/precipitation rates and Atlantic Ocean water inflow; (2) a value of E-P of >1.75 $m^3/m^2/yr$ is required to reproduce a precipitation of thick "2nd step evaporites" (>2000 m) in the deep basins after the major sea-level drawdown, assuming a river discharge of about 7500 m^3/s, comparable to that of the present-day (Struglia et al., 2004; Meijer and Krijgsman, 2005; Gargani and Rigollet, 2007).

In the absence of any alternative, previous studies of the water and salt budget have used present-day hydrological fluxes with E-P ranging between 0.5 and 1 $m^3/m^2/yr$ (Meijer and Krijgsman, 2005). E-P value of 0.9-1 $m^3/m^2/yr$ during the peak of the MES is also suggested from recent climate modelling (Murphy et al., 2009). The higher value of E-P (1.75 $m^3/m^2/yr$) required in our model is consistent with the reconstructed climatic parameters at the time of the MSC indicating lower annual precipitations and higher mean annual temperature than today in the southwest Mediterranean lands (Fauquette et al., 2006; Van Dam, 2006). A higher E-P value than today is also supported by the momentary migration of the subdesertic plants 3° northward of their habitat at the onset of the MSC (Fauquette et al., 2006; Popescu et al., 2007). In the present Dead Sea the rate of evaporation has been measured between 1.25 $m^3/m^2/yr$ and 1.7 $m^3/m^2/yr$ today and in 1944 respectively (Yechieli et al., 1998). With regard to the low precipitation rate (about 0.1 $m^3/m^2/yr$) at the shore of the Dead Sea (Neumann et

al., 2010), an average E-P value of 1.5 $m^3/m^2/yr$ can be considered. Moreover, evaporation rates >2 $m^3/m^2/yr$ have been recorded in various lakes in arid regions (Kotwicki and Isdale, 1991; Abd Ellah, 2009). Therefore 1.75 $m^3/m^2/yr$ is a plausible value for the time of the MSC.

8. Conclusion

Using seismic lines and data from wells in the Gulf of Lions, we showed that detrital prisms started to be deposited in the Provence-Algiers Basin before the deposition of the "2nd step evaporites" and then partly during their deposition. The upper part of these evaporites has been deposited contemporaneously with the formation of a transgressive ravinement surface, during the landward migration of the shoreline. Three successive steps subdividing the peak of the MSC (5.60-5.46 Ma) are defined to characterise the sedimentary pattern observed in seismic reflection and borehole data: step 2-I (5.60-? Ma) corresponds to the deposition of detrital sediment in relation with intensive subaerial erosion immediately after the onset of the fast and major Messinian sea-level drawdown; step 2-II (?-5.46 Ma) is characterised by deposition of evaporites (up to 3 kilometres in thickness) during a slow sea-level rise and associated landward migration of the shoreline; step 2-III is the geologically instantaneous reflooding of the Mediterranean at 5.46 Ma.

This scenario, which details the peak of the MSC, has been numerically modelled for the Western Mediterranean and the expected thickness of evaporites implies that E-P was higher than today in the central basins when they were dried up.

Because of similar observations in the Eastern Mediterranean, this scenario might be applicable for the whole Mediterranean. The key pieces of information required for continuing to improve understanding of the peak of the MSC at the scale of the whole Mediterranean are ground-truth observations of the "2nd step evaporites" and the pre-evaporite lithologies with accurate dating for the corresponding sediments. Recognition of the critical stratigraphic markers identified in the Gulf of Lions and in other Mediterranean basins should allow:

1. more detailed chronostratigraphy of the MSC, leading to comparisons between different basins. In particular, the understanding of the connections between Western and Eastern Mediterranean basins and the role of sills that probably separated these basins is necessary to model the MSC for the whole Mediterranean (Gargani and Rigollet, 2007; Gargani et al., 2008; Leever et al., 2010; Leever et al., 2011; Bache et al., 2012);
2. quantification of vertical movements across the whole Mediterranean that will lead to a better understanding of the behaviour of the lithosphere, its rigidity and response to rapid load variations during the MSC (sedimentary transfers, sea-level variations).
3. new constraints for hydrocarbon generation models for which age and lithology of sedimentary units are critical to assess the petroleum potential of sedimentary basins.

9. Acknowledgments

The authors acknowledge Petroceltic and Total for allowing use of the seismic data. Vaughan Stagpoole (GNS Science) is acknowledged for critical discussions and editing the English.

10. References

Abd Ellah, R.G., 2009. Evaporation rate at Wadi El-Rayan Lake, Egypt. World Applied Sciences Journal 6, 524-528.

Bache, F., 2008. Evolution Oligo-Miocène des marges du micro océan Liguro Provençal. Editions Universitaires Européennes, Saarbrücken.

Bache, F., Olivet, J.L., Gorini, C., Aslanian, D., Labails, C., Rabineau, M., 2010. Evolution of rifted continental margins: the case of the Gulf of Lions (Western Mediterranean Basin). Earth and Planetary Science Letters 292, 345-356.

Bache, F., Olivet, J.L., Gorini, C., Rabineau, M., Baztan, J., Aslanian, D., Suc, J.P., 2009. The Messinian Erosional and Salinity Crises: View from the Provence Basin (Gulf of Lions, Western Mediterranean). Earth and Planetary Science Letters 286, 139-157.

Bache, F., Popescu, S.M., Rabineau, M., Gorini, C., Suc, J.P., Clauzon, G., Olivet, J.L., Rubino, J.L., Melinte-Dobrinescu, M.C., Estrada, F., Londeix, L., Armijo, R., Meyer, B., Jolivet, L., Jouannic, G., Leroux, E., Aslanian, D., Reis, A.T.D., Mocochain, L., Dumurdžanov, N., Zagorchev, I., Lesić, V., Tomić, D., Namik Çağatay, N., Brun, J.P., Sokoutis, D., Csato, I., Ucarkus, G., Çakir, Z., 2012. A two-step process for the reflooding of the Mediterranean Basin after the Messinian Salinity Crisis. Basin Research 24, 125-153.

Barber, P.M., 1981. Messinian subaerial erosion of the Proto-Nile delta. Marine Geology 44, 253-272.

Barr, F.T., Walker, B.R., 1973. Late Tertiary channel system in Northern Lybia and its implications on Mediterranean sea level changes, in: Ryan, W.B.F., Hsü, K.J., al. (Eds.), Initial Reports of Deep Sea Drilling Project, Volume 13. (U.S. Government Printing Office), Washington, pp. 1244-1255.

Benson, R.H., Rakic-El Bied, K., Bonaduce, G., 1991. An important current reversal (influx) in the Rifian Corridor (Morocco) at the Tortonian-Messinian boundary: The end of the Tethys Ocean. Paleoceanography 6, 164-192.

Bertoni, C., Cartwright, J.A., 2007. Clastic depositional systems at the base of the late Miocene evaporites of the Levant region, eastern Mediterranean., in: Schreiber, B.C., Lugli, S., Babel, M. (Eds.), Evaporites through space and time. Geological Society, London, Special Publications, pp. 37-52.

Bessis, F., 1986. Some remarks on the study of subsidence of sedimentary basins. Application to the Gulf of Lions margin (Western Mediterranean). Marine and Petroleum Geology 3, 37-63.

Blanc, P.-L., 2002. The opening of the Plio-Quaternary Gilbraltar Strait : assessing the size of a cataclysm. Geodinamica Acta 15, 303-317.

Blanc, P.L., 2000. Of sills and straits: a quantitaive assessment of the Messinian Salinity Crisis. Deep-Sea Research 47, 1429-1460.

Blanc, P.L., 2006. Improved modelling of the Messinian Salinity Crisis and conceptual implications. Palaeogeography, Palaeoclimatology, Palaeoecology 238, 349-372.

Brolsma, M.J., 1975. Lithostratigraphy and foraminiferal assemblages of the Miocene-Pliocene transitional strata of Capo Rossello and Eraclea Minoa (Sicily, Italy). Konink. Ned. Akad. Van Wetensch. 78, 1-40.

Brun, L., Castet, A., Grosdidier, P., Moreau, P., Prestat, B., Seyve, C., Cussey, R., Fajerwerg, R., Brevart, O., Chennaux, G., Severac, J.P., Barlier, J., Palacios, C., Poumot, C., 1984. Sondage Golfe du Lion profond n°2 GLP2, France, études de laboratoire. SNEA(P) Direction Exploration, Division recherches et applications en géologie, Boussens.

Burrus, J., 1989. Review of geodynamic models for extensional basins; the paradox of stretching in the Gulf of Lions (northwest Mediterranean). Bulletin de la Societe Geologique de France 8, 377-393.

Butler, R.W.H., Lickorish, W.H., Grasso, M., Pedley, H.M., Ramberti, L., 1995. Tectonics and sequence stratigraphy in Messinian basins, Sicily: constraints on the initiation and termination of the Mediterranean salinity crisis. Geological Society of America Bulletin 107, 425-439.

Cherchi, A., Mancin, N., Montadert, L., Murru, M., Teresa Putzu, M., Schiavinotto, F., Verrubbi, V., 2008. The stratigraphic response to the Oligo-Miocene extension in the western Mediterranean from observations on the Sardinia graben system (Italy). Bulletin de la Société géologique de France, 179(3), 267-287.

Chumakov, I.S., 1973. Pliocene and Pleistocene deposits of the Nile Valley in Nubia and Upper Egypt., in: Ryan, W.B.F., Hsü, K.J., al. (Eds.), Initial Reports of Deep Sea Drilling Project, Volume 13. (U.S. Government Printing Office), Washington, pp. 1242-1243.

CIESM (Antón, J., Çağatay, M.N., De Lange, G., Flecker, R., Gaullier, V., Gunde-Cimerman, N., Hübscher, C., Krijgsman, W., Lambregts, P., Lofi, J., Lugli, S., Manzi, V., McGenity, T.J., Roveru, M., Sierro, F.J., & Suc, J.-P.), 2008. Executive Summary, in: Briand, F. (Ed.), The Messinian Salinity crisis from mega-deposits to microbiology - A consensus report. CIESM Workshop Monographs, Monaco, pp. 7-28.

Cita, M.B., 1973. Mediterranean evaporite: paleontological arguments for a deep-basin desiccation model, in: Drooger, C.W. (Ed.), Messinian events in the Mediterranean. North-Holland Publ. Co, Amsterdam, pp. 206-228.

Cita, M.B., Ryan, W.B.F., 1978. Messinian erosional surfaces in the Mediterranean., in: Cita, M.B., Ryan, W.B.F. (Eds.), Marine Geology, p. 366.

Cita, M.B., Wright, R.C., Ryan, W.B.F., 1978. Messinian paleoenvironments, in: Hsü, K.J., Montadert, L., al. (Eds.), Initial Reports of the Deep Sea Drilling Project, Volume 42, Part 1. (U.S. Government Printing Office), Washington, pp. 1003-1035.

Clauzon, G., 1973. The eustatic hypothesis and the pre-Pliocene cutting of the Rhône valley, in: Ryan, W.B.F., Hsü, K.J., al. (Eds.), Initial Reports of Deep Sea Drilling Project, Volume 13. (U.S. Government Printing Office), Washington, pp. 1251-1256.

Clauzon, G., 1974. L'hypothèse eustatique et le creusement prépliocène de la vallée du Rhône. Annales de Geographie 456, 129-140.

Clauzon, G., 1978. The Messinian Var canyon (Provence, Southern France) - Paleogeographic implications. Marine Geology 27, 231-246.

Clauzon, G., 1979. Le canyon messinien de la Durance (Provence, France): Une preuve paléogéographique du bassin profond de dessiccation. Palaeogeography, Palaeoclimatology, Palaeoecology 29, 15-40.

Clauzon, G., 1982. Le canyon messinien du Rhône : une preuve décisive du "dessicated deep-basin model" (Hsü, Cita et Ryan, 1973). Bulletin de la Societe Geologique de France 24, 597-610.

Clauzon, G., 1990. Restitution de l'évolution géodynamique néogène du bassin du Roussillon et de l'unité adjacente des Corbières d'après les données écostratigraphiques et paléogéographiques. Paleobiol. Cont. 17, 125-155.

Clauzon, G., Suc, J.P., Gautier, F., Berger, A., Loutre, M.F., 1996. Alternate interpretation of the Messinian salinity crisis: controversy resolved ? Geology 24, 363-366.

Cravatte, J., Dufaure, P., Prim, M., Rouaix, S., 1974. Les sondages du Golfe du Lion: Stratigraphie, Sédimentologie, Notes et Mémoires n°11. Compagnie Française des Pétroles, Paris, pp. 209-274.

Di Stefano, A., Sturiale, G., 2010. Refinements of calcareous nannofossil biostratigraphy at the Miocene/Pliocene Boundary on the Mediterranean region. Geobios43, 5-20.

Dos Reis, A.T., Gorini, C., Mauffret, A., 2005. Implications of salt-sediment interactions for the architecture of the Gulf of Lions deep-water sedimentary systems, western Mediterranean. Marine and Petroleum Geology 22, 713-746.

Estrada, F., Ercilla, G., Gorini, C., Alonso, B., Vazquez, J., Garcia-Castellanos, D., Juan, C., Maldonado, A., Ammar, A., Elabbassi, M., 2011. Impact of pulsed Atlantic water inflow into the Alboran Basin at the time of the Zanclean flooding. Geo-Marine Letters, 1-16.

Fauquette, S., Bernet, M., Suc, J.-P., Grosjean, A.-S., Guillot, S., van der Beek, P., Jourdan, S., Popescu, S.-M., Jiménez-Moreno, G., Bertini, A., Pittet, B., Tricart, P., Dumont, T., Schwartz, S., Zheng, Z., Roche, E., Pavia, G., Gardien, V., accepted. Quantifying the

Eocene to Pleistocene topographic evolution of the southwestern Alps, France and Italy. Earth and Planetary Science Letters.

Fauquette, S., Suc, J.-P., Bertini, A., Popescu, S.-M., Warny, S., Bachiri Taoufiq, N., Perez Villa, M.-J., Chikhi, H., Subally, D., Feddi, N., Clauzon, G., Ferrier, J., 2006. How much did climate force the Messinian salinity crisis? Quantified climatic conditions from pollen records in the Mediterranean region. Palaeogeography, Palaeoclimatology, Palaeoecology 238, 281-301.

Ferrandini, J., Rossi, P., Ferrandini, M., Farjanel, G., Ginsburg, L., Schuler, M., Geissert, F., 1999. La formation conglomératique du Vazzio près d'Ajaccio (Corse-du-Sud), un témoin des dépôts du Chattien supérieur continental synrift en Méditerranée occidentale. Comptes Rendus de l'Académie des Sciences de Paris, Sciences de la terre et des planètes, 329(4), 271-278.

Garcia-Castellanos, D., Estrada, F., Jiménez-Munt, I., Gorini, C., Fernandez, M., Vergés, J., De Vicente, R., 2009. Catastrophic flood of the Mediterranean after the Messinian salinity crisis. Nature 462, 778-781.

Garcia-Castellanos, D., Villasenor, A., 2011. Messinian Salinity Crisis regulated by competing tectonics and erosion at the Gibraltar arc. Nature 480, 359-363.

García, M., Maillard, A., Aslanian, D., Rabineau, M., Alonso, B., Gorini, C., Estrada, F., 2011. The Catalan margin during the Messinian Salinity Crisis: Physiography, morphology and sedimentary record. Marine Geology 284, 158-174.

Gargani, J., Moretti, I., Letouzet, J., 2008. Evaporite accumulation during the Messinian Salinity Crisis: the Suez Rift case. Geophysical Research Letter 35, L02401.

Gargani, J., Rigollet, C., 2007. Mediterranean Sea level variations during the Messinian salinity crisis. Geophysical Research Letter 34, L10405.

Gautier, F., Clauzon, G., Suc, J.P., Cravatte, J., Violanti, D., 1994. Age and duration of the messinian salinity crisis. Comptes Rendus de l'Académie des Sciences - Series IIA - Earth and Planetary Science 318, 1103-1109.

Gennesseaux, M., Lefebvre, D., 1980. Le Golfe du Lion et le Paléo-Rhône messinien. Géologie Méditerranéenne 7, 71-80.

Gorini, C., 1993. Géodynamique d'une marge passive: le Golfe du Lion (Méditerranée Occidentale). Université Paul Sabatier, Toulouse, p. 256.

Gorini, C., Lofi, J., Duvail, C., Dos Reis, T., Guennoc, P., Le Strat, P., Mauffret, A., 2005. The Late Messinian salinity crisis and Late Miocene tectonism : interaction and consequences on the physiography and post-rift evolution of the Gulf of Lions margin. Marine and Petroleum Geology 22, 695-712.

Govers, R., 2009. Choking the Mediterranean to dehydration: The Messinian salinity crisis. Geology 37, 167-170.

Govers, R., Meijer, P., Krijgsman, W., 2009. Regional isostatic response to Messinian Salinity Crisis events. Tectonophysics 463, 109-129.

Guennoc, P., Gorini, C., Mauffret, A., 2000. Histoire géologique du Golfe du Lion et cartographie du rift oligo-aquitanien et de la surface messinienne. Géologie de la France 3, 67-97.

Haq, B.U., Hardenbol, J., Vail, P.R., 1987. Chronology of Fluctuating Sea Levels Since the Triassic. Science 235, 1156-1167.

Hardie, L.A., Lowenstein, T.K., 1985. Criteria for recognition of ephemeral salt-pan facies in halite evaporites. Sedimentology 32, 627-644.

Hardie, L.A., Lowenstein, T.K., 2004. Did the Mediterranean sea dry out during the Miocene? A reassessment of the evaporite evidence from DSDP legs 13 and 42A cores. Journal of Sedimentary Research 74, 453-461.

Hilgen, F.J., Langereis, C.G., 1993. A critical re-evaluation of the Miocene-Pliocene boundary as defined in Mediterranean. Earth and Planetary Science Letters 118, 167-179.

Hsü, K.J., 1972a. Origin of saline giants: a critical review after the discovery of the Mediterranean Evaporites. Earth-Science Reviews 8, 371-396.

Hsü, K.J., 1972b. When the Mediterranean dried up. Sci. Am. 227, 44-51.

Hsü, K.J., 1973. The desiccated deep-basin model for the Messinian events, in: Drooger, C.W. (Ed.), Messinian events in the Mediterranean. North-Holland Publ. Co., Amsterdam, pp. 60-67.

Hsü, K.J., Bernoulli, D., 1978. Genesis of the Thethys and the Mediterranean, in: Hsü, K.J., Montadert, L., al. (Eds.), Initial Reports of the Deep Sea Drilling Project, Volume 42, Part 1. (U.S. Government Printing Office), Washington, pp. 943-950.

Hsü, K.J., Cita, M.B., Ryan, W.B.F., 1973a. The origin of the Mediterranean evaporites, in: Ryan, W.B.F., Hsü, K.J., al. (Eds.), Initial Reports of Deep Sea Drilling Project. U.S. Government Printing Office, Washington, pp. 1203-1231.

Hsü, K.J., Montadert, L., Bernoulli, D., Cita, M.B., Erickson, A.J., Garrison, R.E., Kidd, R.B., Mélières, F., Müller, C., Wright, R., 1977. History of the Mediterranean salinity crisis. Nature 267, 399-403.

Hsü, K.J., Ryan, W.B.F., Cita, M.B., 1973b. Late Miocene Desiccation of the Mediterranean. Nature (London) 242, 240-244.

Hunt, D., Tucker, M.E., 1992. Stranded parasequences and the forced regressive wedge systems tract: deposition during base-level fall. Sedimentary Geology 81, 1-9.

Ianev, R.S., Bordas-Le Floch, N., Underhill, J.R., Bunt, R.J.W., 2007. The role of active structural growth in controlling deep-water reservoir systems and petroleum prospectivity in the confined Gulf of Lion Basin, Western Mediterranean, AAPG Annual convention, Long Beach, California.

Just, J., Hübscher, C., Betzler, C., Lüdmann, T., Reicherter, K., 2011. Erosion of continental margins in the Western Mediterranean due to sea-level stagnancy during the Messinian Salinity Crisis. Geo-Marine Letters 31, 51-64.

Kotwicki, V., Isdale, P., 1991. Hydrology of Lake Eyre, Australia: El Nino link. Palaeogeography, Palaeoclimatology, Palaeoecology 84, 87-98.

Krijgsman, W., Hilgen, F.J., Raffi, I., Sierro, F.J., Wilson, D.S., 1999a. Chronology, causes and progression of the Messinian salinity crisis. Nature 400, 652-655.

Krijgsman, W., Langereis, C.G., Zachariasse, W.J., Boccaletti, M., Moratti, G., Gelati, R., Iaccarino, S., Papani, G., Villa, G., 1999b. Late Neogene evolution of the Taza-Guercif Basin (Riftian Corridor, Morocco) and implications for the Messinian salinity crisis. Marine Geology 153, 147-160.

Krijgsman, W., Meijer, P.T., 2008. Depositional environments of the Mediterranean "Lower Evaporites" of the Messinian salinity crisis: Constraints from quantitative analyses. Marine Geology 253, 73-81.

Leever, K.A., Matenco, L., Garcia-Castellanos, D., Cloetingh, S., 2011. The evolution of the Danube gateway between Central and Eastern Paratethys (SE Europe): insight from numerical modelling of the causes and effects of connectivity between basins and its expression in the sedimentary record. . Tectonophysics 502, 175-195.

Leever, K.A., Matenco, L., Rabagia, T., Cloetingh, S., Krijgsman, W., Stoica, M., 2010. Messinian sea level fall in the Dacic Basin (Eastern Paratethys): palaeogeographical implications from seismic sequence stratigraphy. Terra Nova 22, 12-17.

Lefebvre, D., 1980. Evolution morphologique et structurale du Golfe du Lion. Essai de traitement statistique des données. Université de Paris 6, Paris, p. 163.

Lofi, J., Berné, S., 2008. Evidence for pre-messinian submarine canyons on the Gulf of Lions slope (Western Mediterranean). Marine and Petroleum Geology 25, 804-817.
Lofi, J., Deverchère, J., Gaullier, V., Gillet, H., Guennoc, P., Gorini, C., Loncke, L., Maillard, A., Sage, F., Thinon, I., 2011. Seismic atlas of the Messinian salinity crisis markers in the offshore Mediterranean domain. CCGM & Mém. Soc. géol. Fr., n.s. 179, 72 pp.
Lofi, J., Gorini, C., Berné, S., Clauzon, G., Dos Reis, A.T., Ryan, W.B.F., Steckler, M.S., 2005. Erosional processes and paleo-environmental changes in the Western Gulf of Lions (SW France) during the Messinian Salinity Crisis. Marine Geology 217, 1-30.
Lofi, J., Rabineau, M., Gorini, C., Berne, S., Clauzon, G., de, C.P., dos, R.A.T., Mountain, G.S., Ryan, W.B.F., Steckler, M.S., Fouchet, C., 2003. Plio-Quaternary prograding clinoform wedges of the western Gulf of Lion continental margin (NW Mediterranean) after the Messinian salinity crisis. Marine Geology 198, 289-317.
Loget, N., Van den Driessche, J., Davy, P., 2005. How did the Messinian Salinity Crisis end? Terra Nova 17.
Lourens, L.J., Hilgen, F.J., Laskar, J., Shackleton, N.J., Wilson, D., 2004. The Neogene Period, in: Gradstein, F.M., Ogg, J., Smith, A. (Eds.), A Geological Time Scale. Cambridge University Press, Cambridge, pp. 409-440.
Manzi, V., Gennari, R., Hilgen, F.J., Krijgsman, W., Lugli, S., Roveri, M., Sierro, F.J., 2013. Age refinement of the Messinian salinity crisis onset in the Mediterranean. Terra Nova 26, 315-322.
Mauffret, A., Durand de Grossouvre, B., Dos Reis, A.T., Gorini, C., Nercessian, A., 2001. Structural geometry in the eastern Pyrenees and western Gulf of Lion (Western Mediterranean). Journal of Structural Geology 23, 1701-1726.
Meijer, P., 2006. A box model of the blocked-outflow scenario for the Messinian Salinity Crisis. Earth and Planetary Science Letters 248, 471-479.
Meijer, P., Krijgsman, W., 2005. A quantitative analysis of the desiccation and re-filling of the Mediterranean during the Messinian Salinity Crisis. Earth and Planetary Science Letters 240, 510-520.
Meulenkamp, J.E., Sissingh, W., 2003. Tertiary palaeogeography and tectonostratigraphic evolution of the Northern and Southern Peri-Tethys platforms and the intermediate domains of the Agrican−Eurasian convergent plate boundary zone. Palaeogeography, Palaeoclimatology, Palaeoecology 196, 209-228.
Miller, K.G., Mountain, G.S., Wright, J.D., Browning, J.V., 2011. A 180-MillioYear Record of Sea Level and Ice Volume Variations from Continental Margin and Deep-Sea Isotopic Records. Oceanography 24(2), 40-53.
Mitchum, R.M., Vail, P.R., Sangree, J.B., 1977. Seismic stratigraphy and global changes of sea level, part 6: Stratigraphic Interpretation of Seismic Reflection Patterns in Depositional Sequences, in: Payton, C.E. (Ed.), Seismic stratigraphy - Application to hydrocarbon exploration. American Association of Petroleum Geologists, Tulsa, pp. 117-133.
Montadert, L., Letouzey, J., Mauffret, A., 1978. Messinian event : seismic evidence, in: Hsü, K.J., Montadert, L., al (Eds.), Initial Reports of the Deep Sea Drilling Project, Volume 42, Part 1. (U.S. Government Printing Office), Washington, pp. 1037-1050.
Montadert, L., Nicolaides, S., Semb, P.H., Lie, Ø., 2011. Petroleum systems offshore Cyprus, in: Marlow, L., Kedall, C., Yose, L. (Eds.), Petroleum Systems of the Tethyan Region. American Association of Petroleum Geologists.
Murphy, L., Kirk-Davidoff, D.B., Mahowald, N., Otto-Bliesner, B.L., 2009. A numerical study of the climate response to lowered Mediterranean Sea level during the Messinian Salinity Crisis. Palaeogeography, Palaeoclimatology, Palaeoecology 279, 41-59.

Neumann, F.H., Kagan, E.J., Leroy, S.A.G., Baruch, U., 2010. Vegetation history and climate fluctuations on a transect along the Dead Sea west shore and their impact on past societies over the last 3500 years. Journal of Arid Environments 74, 756-764.

Pautot, G., Le Cann, C., Coutelle, A., Mart, Y., 1984. Morphology and extension of the evaporitic structures of the Liguro-Provencal basin: new sea-beam data. Marine Geology 55, 387-409.

Popescu, S.M., Dalesme, F., Jouannic, G., Escarguel, G., Head, M.J., Melinte-Dobrinescu, M.C., Sütő-Szentai, M., Bakrac, K., Clauzon, G., Suc, J.P., 2009. *Galeacysta etrusca* complex, dinoflagellate cyst marker of Paratethyan influxes into the Mediterranean Sea before and after the peak of the Messinian Salinity Crisis. Palynology 33, 105-134.

Popescu, S.M., Suc, J.P., Melinte, M., Clauzon, G., Quillévéré, F., Sütő-Szentai, M., 2007. Earliest Zanclean age for the Colombacci and uppermost Di tetto formations of the "latest Messinian" northern Apennines: New palaeoenvironmental data from the Maccarone section (Marche Province, Italy). Geobios 40, 359-373.

Rabineau, M., Berné, S., Aslanian, D., Olivet, J.-L., Joseph, P., Guillocheau, F., Bourillet, J.-F., Ledrezen, E., Granjeon, D., 2005. Sedimentary sequences in the Gulf of Lion: a record of 100,000 years climatic cycles. Marine and Petroleum Geology 22, 775-804.

Raffi, I., Backman, J., Fornaciari, E., Pälike, H., Rio, D., Lourens, L., Hilgen, F., 2006. A review of calcareous nannofossil astrobiochronology encompassing the past 25 million years. Quaternary Science Reviews 25, 3113-3137.

Rizzini, A., Vezzani, F., Cococcetta, V., Milad, G., 1978. Stratigraphy and sedimentation of a Neogen-Quaternary section in the Nile delta aera (A.R.E.). Marine Geology 27, 327-348.

Rouchy, J.M., Caruso, A., 2006. The Messinian salinity crisis in the Mediterranean basin: A reassessment of the data and an integrated scenario. Sedimentary Geology 188, 35-67.

Roveri, M., Lugli, S., Manzi, V., Schreiber, B.C., 2008a. The Messinian Sicilian stratigraphy revisited: toward a new scenario for the Messinian Salinity Crisis. Terra Nova 20, 483-488.

Roveri, M., Manzi, V., 2006. The Messinian salinity crisis: Looking for a new paradigm? Palaeogeography, Palaeoclimatology, Palaeoecology 238, 386-398.

Roveri, M., Manzi, V., Gennari, R., Iaccarino, S.M., Lugli, S., 2008b. Recent advancements in the Messinian stratigraphy of Italy and their Mediterranean-scale implications. Bollettino della Società Paleontologica Italiana 47, 71-85.

Ryan, W.B.F., 1973. Geodynamic implications of the Messinian crisis of salinity, in: Drooger, D.W. (Ed.), Messinian events in the Mediterranean. Elsevier, Amsterdam, pp. 26-38.

Ryan, W.B.F., 2008. Modelling the magnitude and timing of evaporative drawdown during the Messinian salinity Crisis. Stratigraphy 5, 227-243.

Ryan, W.B.F., 2009. Decoding the Mediterranean salinity crisis. Sedimentology 56, 95-136.

Ryan, W.B.F., Cita, M.B., 1978. The nature and distribution of Messinian erosional surface-indication of a several kilometer-deep Mediterranean in the Miocene. Marine Geology 27, 193-230.

Ryan, W.B.F., Hsü, K.J., al., 1973. Initial Reports of the Deep Sea Drilling Project, Volume XIII. (U.S. Government Printing Office), Washington.

Savoye, B., Piper, D.J.W., 1991. The Messinian event on the margin of the Mediterranean Sea in the Nice area, southern France. Marine Geology 97, 279-304.

Stampfli, G.M., Höcker, C.F.W., 1989. Messinian palaeorelief from a 3-D seismic survey in the Tarraco concession area (Spanish Mediterranean Sea). Geol. Mijnb 68, 201-210.

Steckler, M.S., Watts, A.B., 1980. The Gulf of Lion: subsidence of a young continental margin. Nature 287, 425-429.

Struglia, M.V., Mariotti, A., Filograsso, A., 2004. River discharge into the Mediterranean Sea: climatology and aspects of observed variability. Journal of Climate 17, 4740-4751.
Suc, J.-P., Clauzon, G., Bessedik, M., Leroy, S., Zheng, Z., Drivaliari, A., Roiron, P., Ambert, P., Martinell, J., Doménech, R., Matias, I., Julià, R., Anglada, R., 1992. Neogene and Lower Pleistocene in Southern France and Northeastern Spain. Mediterranean environments and climate. Cahiers de Micropaleontologie 7(1-2), 165-186.
Vail, P.R., Mitchum, R.M., Todd, R.G., Widmier, J.M., Thompson, S., Sangree, J.B., Bubb, J.N., Hatlelid, W.G., 1977. Seismic stratigraphy and global changes of sea-level. Seismic stratigraphy-applications to hydrocarbon exploration. Memoir 26. American Association of Petroleum Geologists, Tulsa.
Van Couvering, J.A., Castradori, D., Cita, M.B., Hilgen, F.J., Rio, D., 2000. The base of the Zanclean Stage and of the Pliocene Series. Episodes 23, 179-187.
Van Dam, J.A., 2006. Geographic and temporal patterns in the late Neogene (12-3 Ma) aridification of Europe: The use of small mammal as paleoprecipitation proxies. 238, 190-218.
Warny, S.A., Bart, P.J., Suc, J.P., 2003. Timing and progression of climatic, tectonic and glacioeustatic influences on the Messinian Salinity Crisis. Palaeogeography, Palaeoclimatology, Palaeoecology 202, 59-66.
Yechieli, Y., Gavrieli, I., Berkowitz, B., Ronen, D., 1998. Will the Dead Sea die? Geology 26, 755-758.

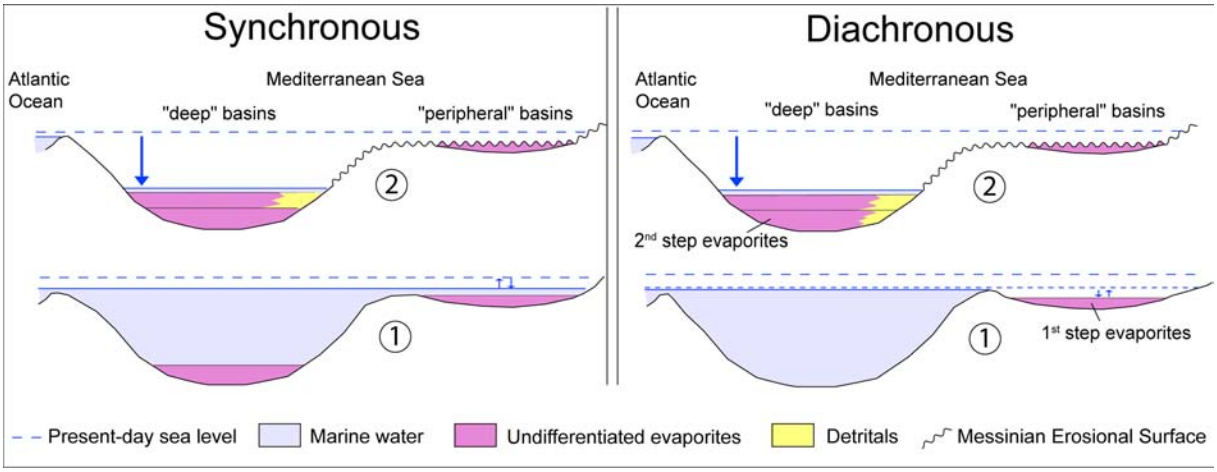

Figure 1. The synchronous and diachronous scenarios for the deposition of the Messinian evaporites in the Mediterranean Sea. In the synchronous scenario phase 1 corresponds to a series of limited sea-level fall and rise leading to evaporite deposition in both the central and peripheral basins; i.e. at variable sea levels. Phase 2 (*i.e.* the peak of the MSC) is characterized by a large sea level drop, evaporite deposition in the central basins, and subaerial erosion of the margins. In the diachronous scenarios evaporites were only deposited in the peripheral basins during phase 1 and in the central basins during phase 2.

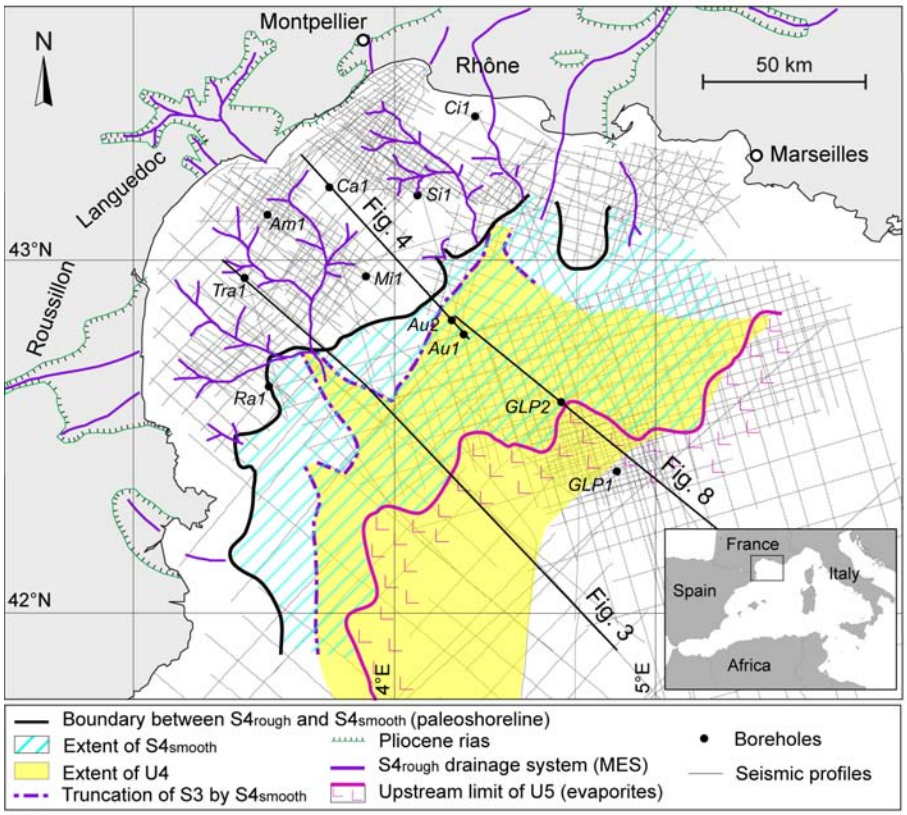

Figure 2. Map showing the data used for this study and the location of Messinian seismic markers in the Gulf of Lions. Landward limit of U5 (evaporites) is deduced from the landward limit of the listric faults. Boreholes: *Ca1*, Calmar1; *Ci1*, Cicindelle1; *Am1*, Agde Maritime1; *Si1*, Sirocco1; *Mi1*, Mistral1; *Tra1*, Tramontane1; *Ra1*, Rascasse1; *Au1*, Autan1; *Au2*, Autan2; *GLP1*, Golfe du Lion Profond 1; *GLP2*, Golfe du Lion Profond 2.

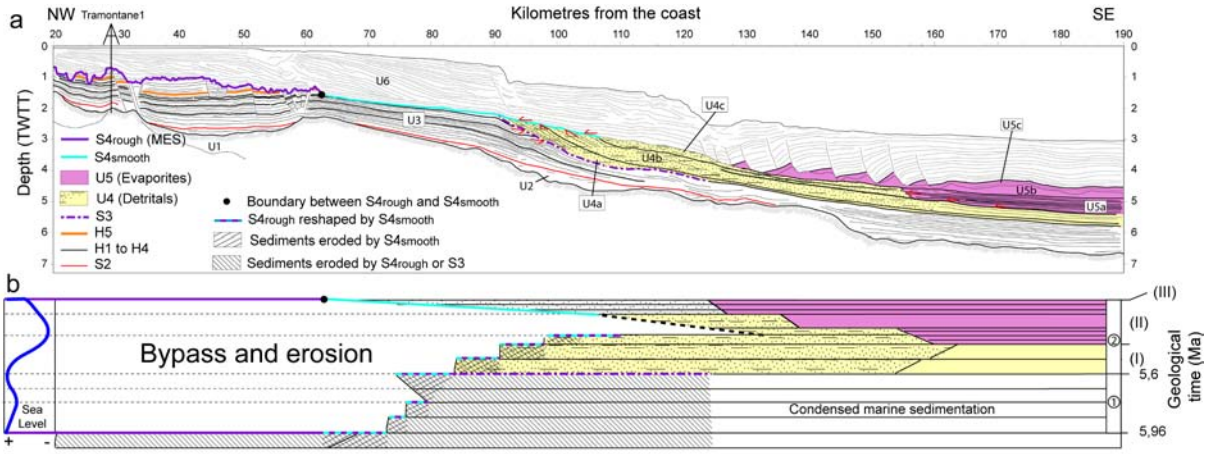

Figure 3. Sedimentary and morphological evolution of the Gulf of Lions from the margin to basin. (a) Line drawing of seismic cross-sections highlighting the markers of the MSC (location on Fig. 1). (b) Chronostratigraphic chart based on seismic interpretations assuming the deposition of a significant part of evaporites after the major sea-level fall and during a landward migration of the shoreline. Subdivisions of the MSC: 1, First phase leading to evaporite deposition in the peripheral basins ("1st step evaporites") after a limited sea level fall; 2, Second phase (*i.e.* the peak of the MSC) characterised by a significant sea level drop, evaporite deposition in the deep basins ("2nd step evaporites"), and subaerial erosion of the margins. Subdivisions of the peak of the MSC: step 2-I, detrital deposition in the central

basins during the significant sea level drop; step 2-II, central evaporites deposited and S4smooth created during the landward migration of the shoreline; step 2-III, rapid reflooding.

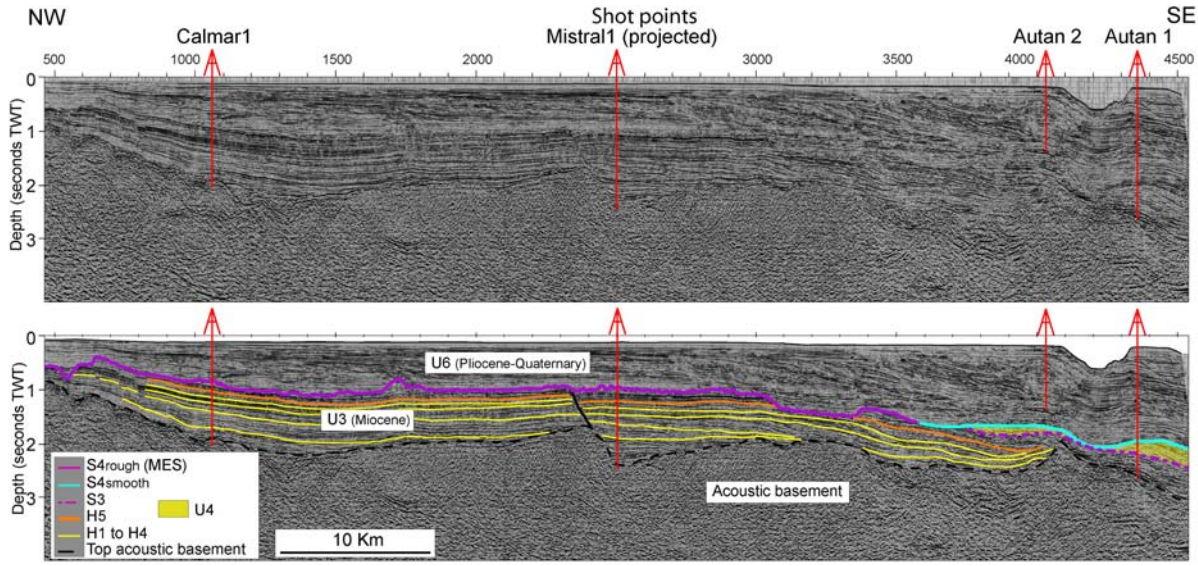

Figure 4. Uninterpreted and interpreted seismic profile across the Gulf of Lions shelf (LRM 28) showing the position of seismic reflectors H1 to H5 beneath U4. A Serravallian/Tortonian age for H5 leads to a younger age for the deposition of U4. Location of seismic profiles on Fig. 2.

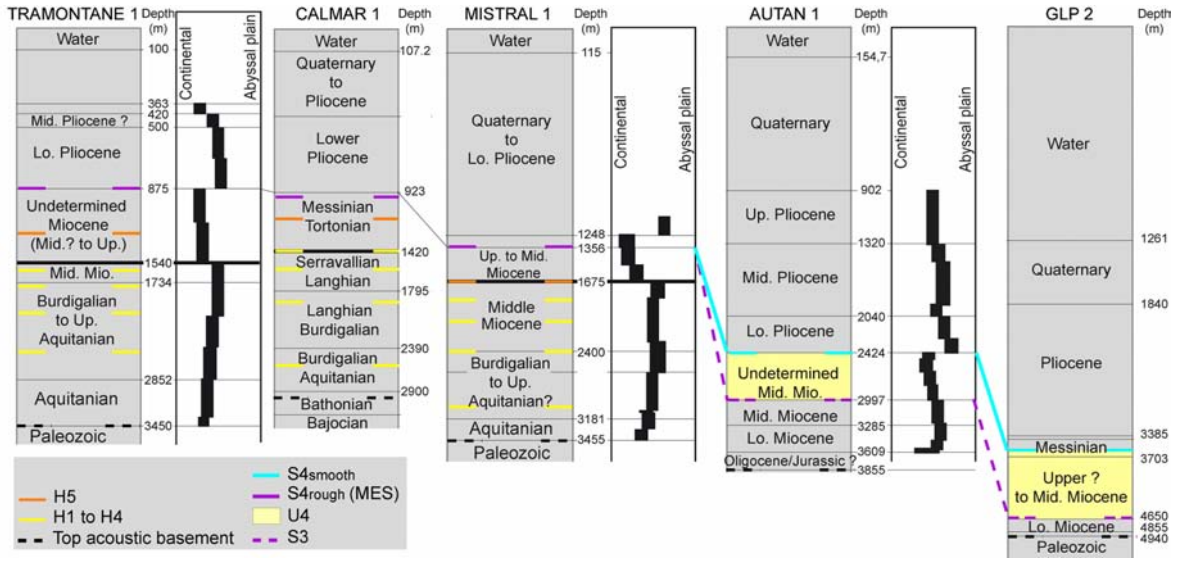

Figure 5. Stratigraphic correlation between wells Tramontane 1, Calmar 1, Mistral 1 (shelf) and Autan 1 and GLP 2 (slope) in the Gulf of Lions (Location on Fig. 2). Stratigraphic boundaries and interpretation of depositional environments come from Cravatte et al. (1974), Brun et al. (1984) and Guennoc et al. (2000). The bold line corresponds to a clear change in depositional environment. Position of the seismic units and unconformities identified in this study is deduced from two-way time – depth relationships (Supplementary Figure 2). Depths are measured depths in meters below Kelly Bushing (mMDKB).

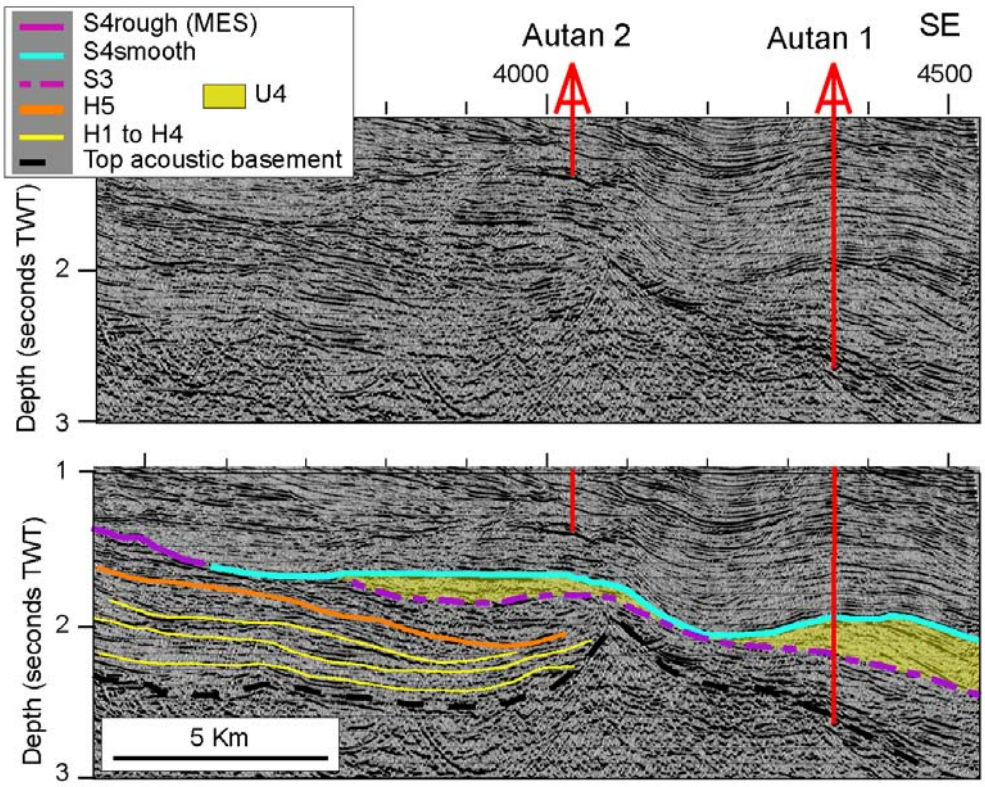

Figure 6. Zoom of Figure 4 showing the stratal relationship between U3 and U4 and the unconformity S3 that separates these units. Seismic reflectors H1 to H5 are older than U4. A Serravallian/Tortonian age for H5 leads to a younger age for the deposition of U4.

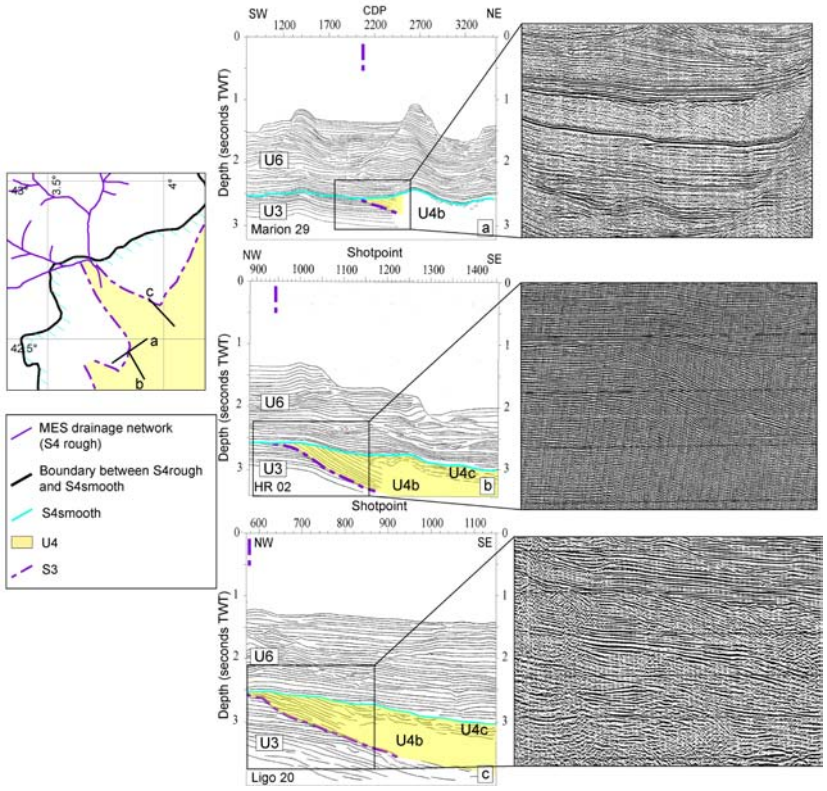

Figure 7. Seismic profiles showing the stratal relationship between U3 and U4 and the unconformity S3 that separates these units. U3 is truncated by S3 and U4 is clearly younger than U3.

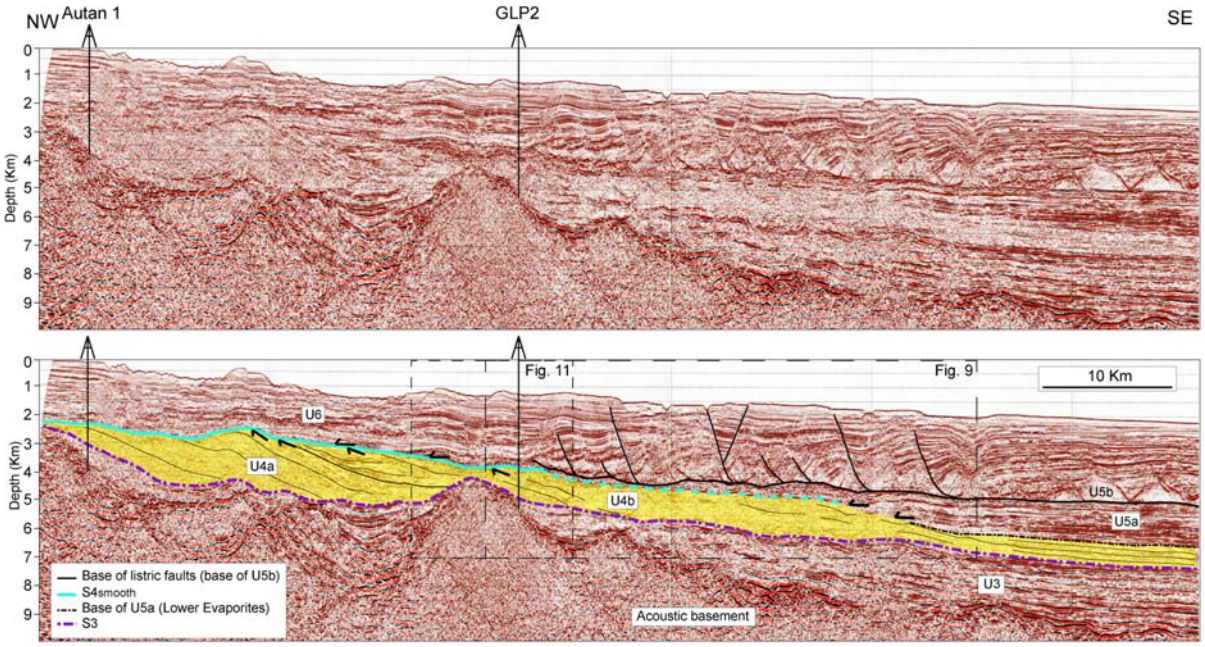

Figure 8. Uninterpreted and interpreted seismic profile across the Gulf of Lions showing the transition from the Miocene shelf (U3) to the evaporite layers (U5). U4 is represented in yellow. S4smooth is characterised by underlying erosional truncations and overlying onlap terminations. Location of seismic profiles on Fig. 2.

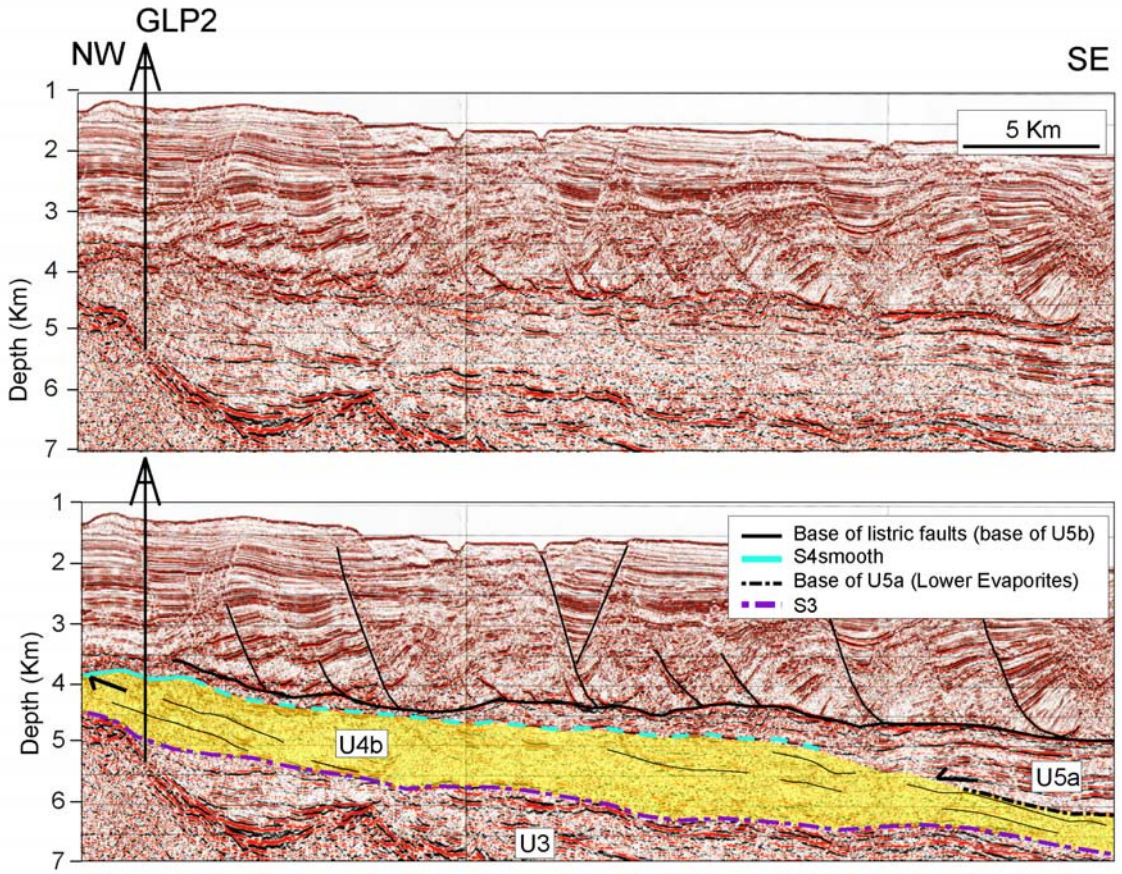

Figure 9. Zoom of Figure 8 showing the transition between U4b and U5a. The evaporitic unit drilled in GLP2 can be correlated with the upper part of U5a.

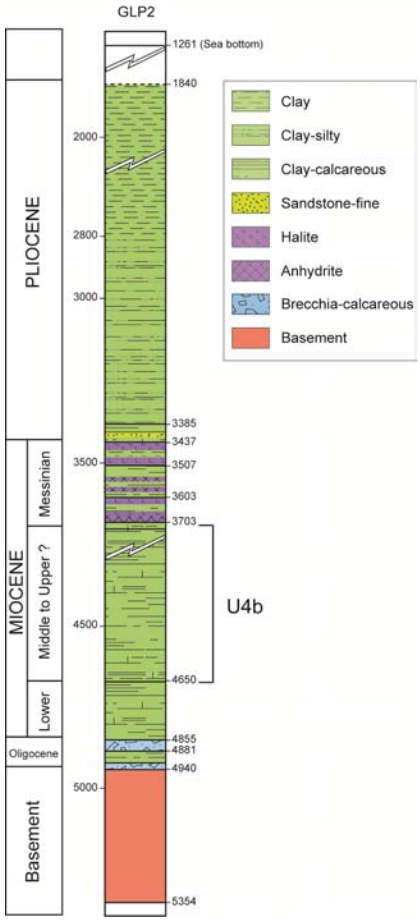

Figure 10. Stratigraphic log of GLP 2 showing the evaporites interval between 3437 and 3703 m and the interval corresponding to seismic unit U4b between 3703 m and 4650 m. Micropaleontologic assemblages are generally poor and non-characteristics between 3703 m and 4650 m (Brun et al., 1984). We interpret this interval as a possible product of the erosion that occurred on the slope during the peak of the MSC. Stratigraphic boundaries come from Brun et al. (1984). Depths are measured depths in meters below Kelly Bushing (mMDKB).

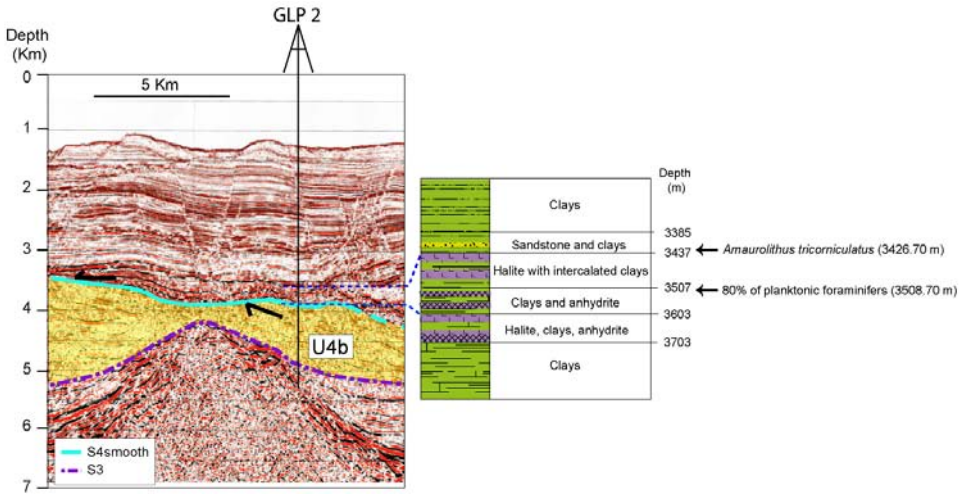

Figure 11. Zoom of Figure 8 showing onlap configuration of the strata that overlies S4smooth. These strata correspond with the evaporitic unit drilled by well GLP2 (3703 – 3437 m depth). The (52 m thick) overlying sandstones and clays (3437 – 3385 m depth) are indistinct on the seismic profile. Depths are measured depths in meters below Kelly Bushing (mMDKB).

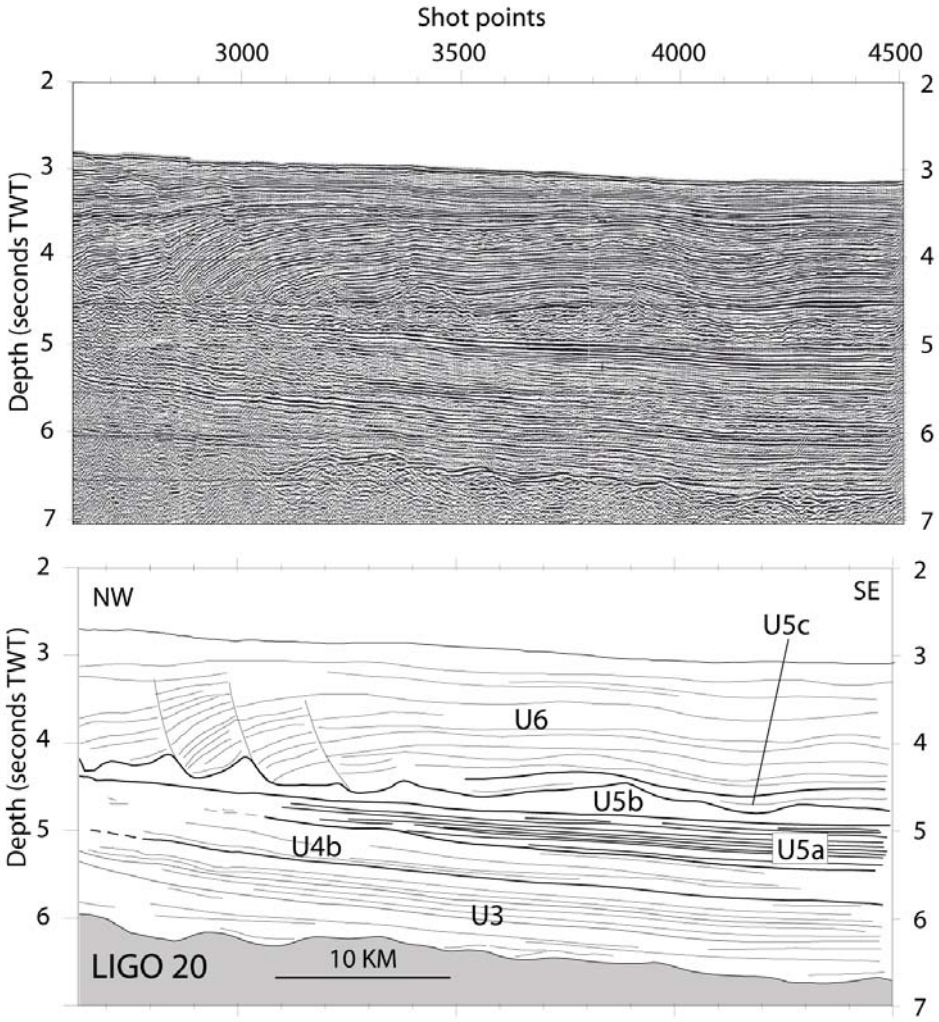

Figure 12. Seismic profile Ligo20 used in Figure 3 showing the onlap configuration of U5a on U4b.

Figure 13. Observations and photographs made by one of us (J.-L.R.) during a dive using the *Cyana* submersible (cruise MONICYA in 1989, dive 72) in the sub-marine Cirque Marcel (western slope) offshore Nice (Southeastern France) corresponding to the proximal part of the Messinian lowstand detritic fan. The vertical scale (10 cm) is valid for the photographs B, C and D. A, Location map of the dive (within the box). Bathymetry is from Pautot et al. (1984). Map of Messinian evaporites and detritic fan is from Savoye and Piper (1991). 1, Messinian evaporites; 2, Messinian lowstand detritic fan in extension of the Messinian valley drawn onshore. B, Cross bedded sandstones described by Savoye and Piper (1991) at 2150 m bsl, underlying fluvial conglomerates. C, Fluvial conglomerates at 2020 m bsl with imbricated clasts of the proximal part of the lowstand detritic cone with a rubefacted matrix. D, Thinly bedded silty turbidites of the distal bottomset beds of the Var Zanclean Gilbert-type fan delta observed at 1940 m bsl.

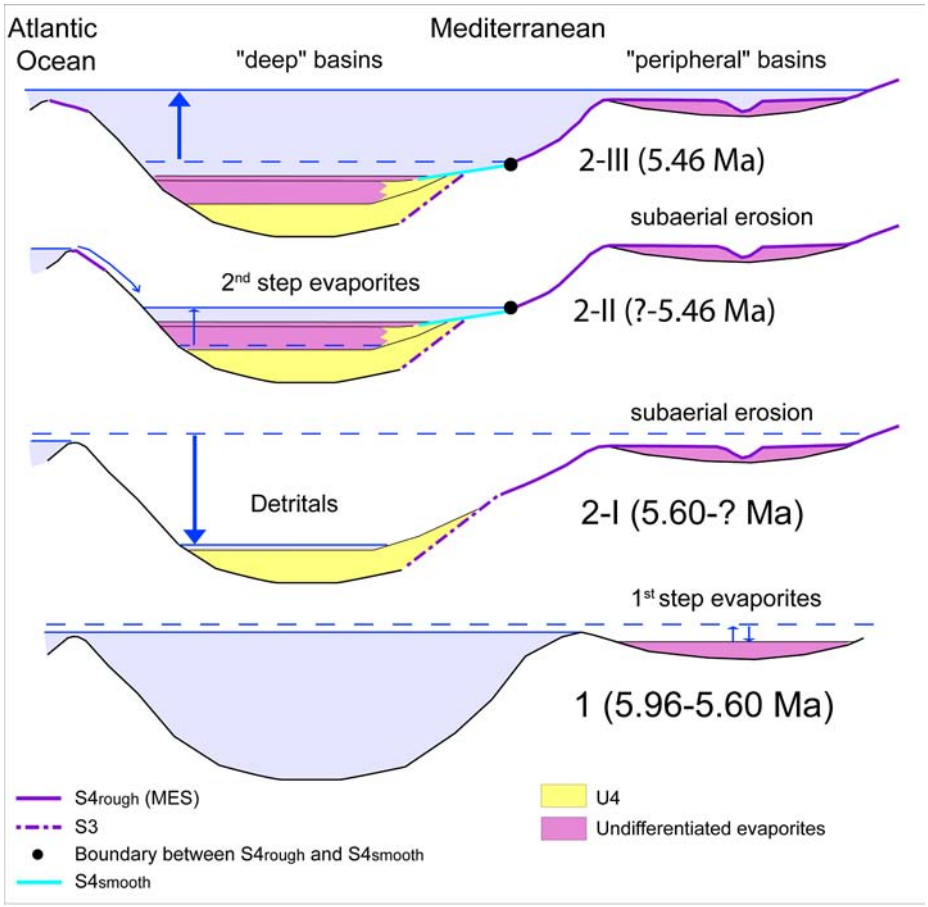

Figure 14. Proposed scenario of the MSC interpreted from the available onshore data for the peripheral basins (see Bache et al., 2012) and from seismic interpretation in the Gulf of Lions (Bache et al., 2009; this study). Subdivisions of the MSC: 1, First phase leading to evaporite deposition in the peripheral basins ("1st step evaporites") after a limited sea level fall; 2, Second phase (*i.e.* the peak of the MSC) characterised by a significant sea level drop, evaporite deposition in the deep basins ("2nd step evaporites"), and subaerial erosion of the margins. Subdivisions of the peak of the MSC: step 2-I, detrital deposition in the deep basins during the significant sea level drop; step 2-II, deep evaporites deposited and S4smooth created during the landward migration of the shoreline; step 2-III, rapid reflooding.

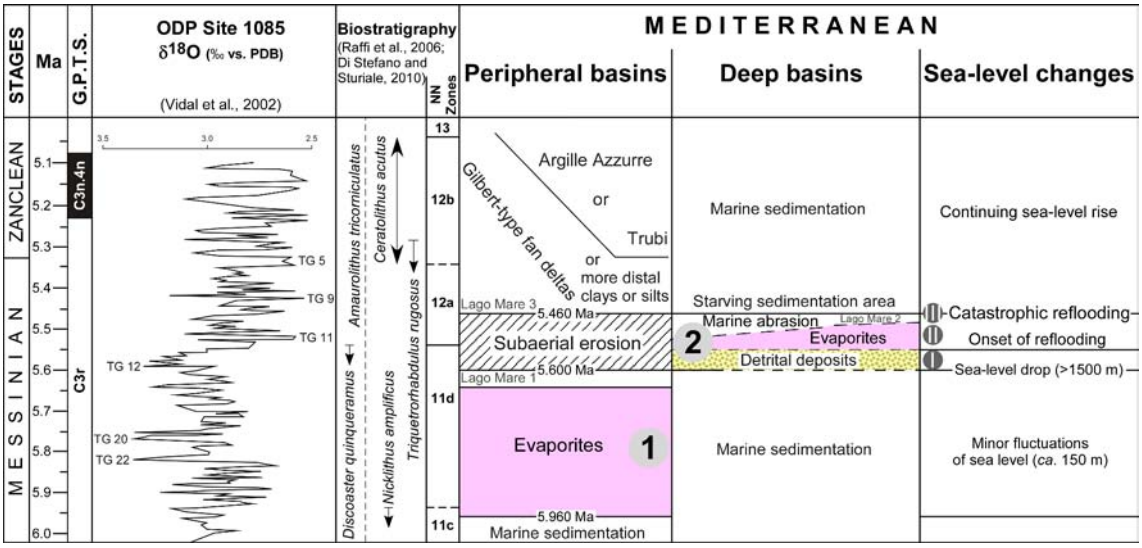

Figure 15. Chronology of events which affected the Mediterranean peripheral (including the Sicilian Caltanissetta Basin and the Apennine Foredeep) and deep basins with respect to sea-level changes (modified from Bache et al., 2012). Subdivisions of the MSC: 1, First phase leading to evaporite deposition in the peripheral basins ("1st step evaporites") after a limited sea-level fall; 2, Second phase (*i.e.* the peak of the MSC) characterised by a significant sea level drop, evaporite deposition in the deep basins ("2nd step evaporites"), and subaerial erosion of the margins. Subdivisions of the peak of the MSC: step 2-I, detrital deposition in the deep basins during the significant sea-level drop; step 2-II, central evaporites deposited and S4smooth created during the landward migration of the shoreline; step 2-III, rapid reflooding.

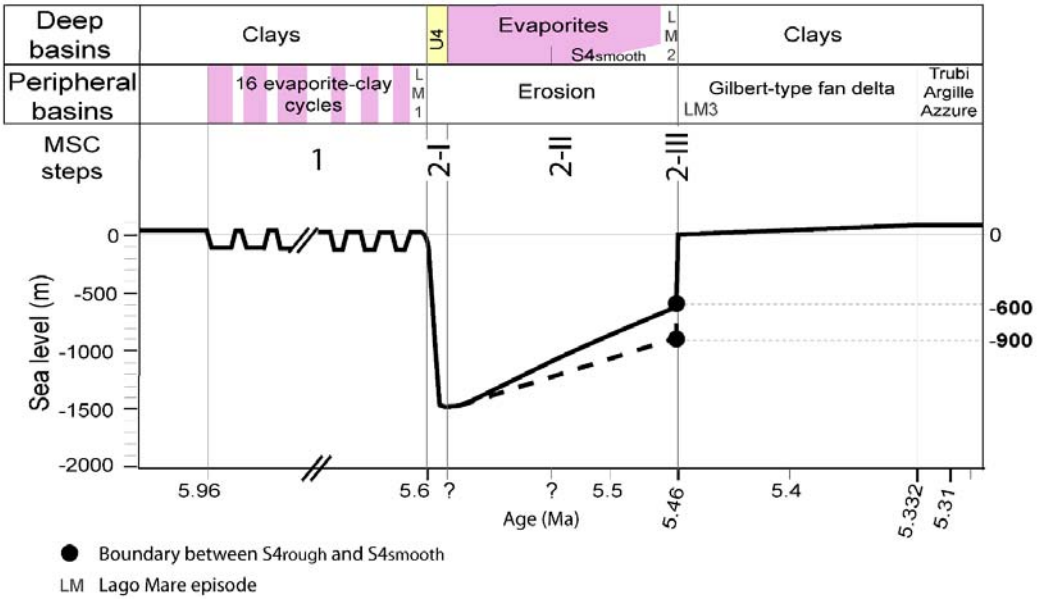

Figure 16. Variation of the Mediterranean Sea level in the Gulf of Lions between 6 and 5.30 Ma encompassing the MSC (augmented from Bache et al. (2012)). Successive major changes are estimated with respect to present-day sea level (0 m). The initial position of the paleoshoreline just before the rapid reflooding (step 2-III) has been estimated between 600 and 900 m below the present day sea level by Bache et al. (2012). The rapid increase in water depth during step 2-III was thus between 600 and 900 m. Solid and dashed black lines are constrained by an increase of 600 m and 900 m respectively. Subdivisions of the MSC shown on Fig. 14.

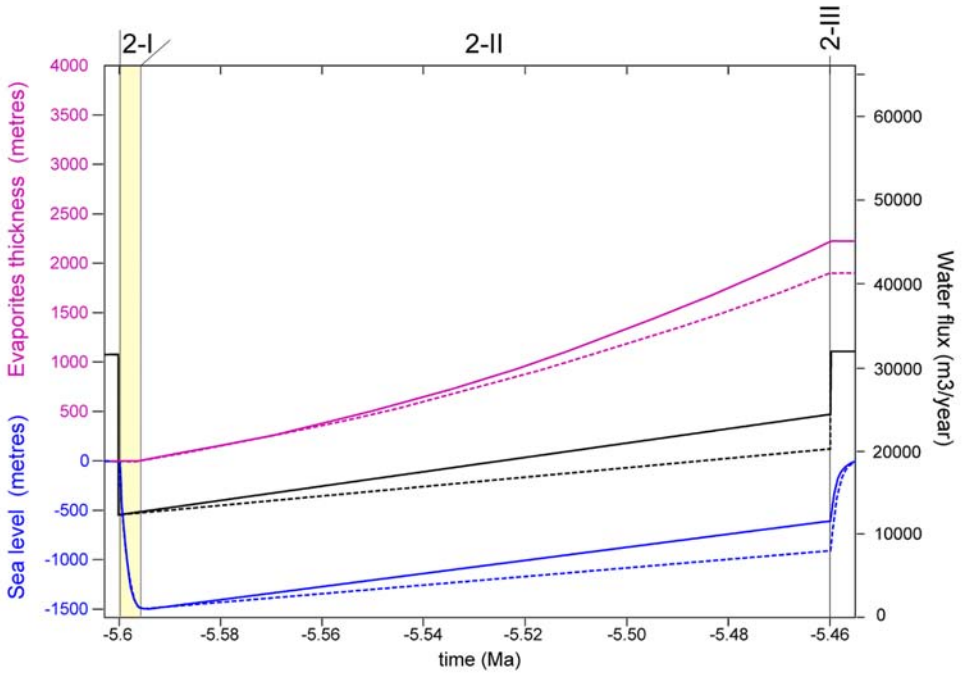

Figure 17. Numerical simulations that predict precipitation of central basin evaporites after the main Messinian sea level fall. Variation of sea level is in blue and that of water budget in black. The resulting simulation of evaporite thickness is in purple. Solid and dashed lines are constrained by the initial position of the paleoshoreline just before step 2-III, respectively at 600 m and 900 m below the present sea level (Bache et al., 2012)**.** The geometry of the basins is identical to that previously modelled by (Meijer and Krijgsman, 2005). Evaporites begin to precipitate when water salinity reaches 130g/l (Meijer and Krijgsman, 2005; Gargani et al., 2008). The water budget is calculated using river and Atlantic Ocean flow as well as precipitation and evaporation (Gargani and Rigollet, 2007). The evaporation – precipitation (E-P) value that is the most compatible with our observations is 1.75 $m^3/m^2/yr$.

Seismic surveys	Wells	Dive
MEDS 76		
MAP 77		
LIGO 80	Agde Maritime 1	
MDT 80	Autan 1	
HR 80	Autan 2	
GL 80	Calmar 1	Cruise
HR81	Cicindelle 1	MONICYA
LIGO81	GLP 1	(1989)
GL 81	GLP 2	Dive 72
MF 82	Mistral 1	
RM 84	Rascasse 1	
SW 84	Sirocco 1	
ECORS 88	Tramontane 1	
LRM 96		
RM 09 (only RM 208)		

Supplementary Figure 1. Data used for this study

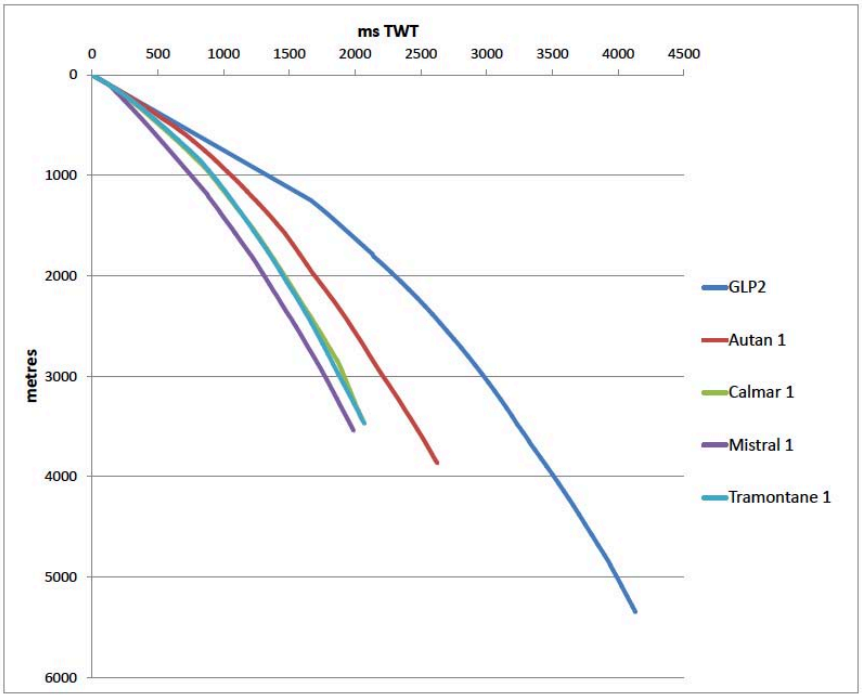

Supplementary Figure 2. Time/depth relationships used in this study.

This study	Dos Reis et al., 2005	Gorini et al., 2005	Lofi et al., 2005	Lofi and Berné, 2008	Bache et al., 2009	Lofi et al., 2011	Bache et al., 2012
Fig. 3			**Fig. 8**	**Fig. 2**	**Fig. 3**	**Fig. 3.4**	**Fig. 5**
U6	*Pliocene - Su*	*Pliocene-Quaternary*	*Plio-Quaternary*	PP	*Pliocene-Quaternary*	*PQ*	g (*Pliocene-Quaternary*)
S4rough	*Messinian unconformity*	*Messinian unconformity*	*MES (Messinian Erosional Surface)*	MES (Margin Erosional Surface)	Rough erosion surface	MES (Margin Erosion Surface)	f (MES, Margin Erosional Surface)
S4smooth	*Messinian unconformity*	*Messinian unconformity*	*MES (Messinian Erosional Surface)*	MES (Margin Erosional Surface)	Smooth erosion surface	MES (Margin Erosion Surface)	e (planation surface)
U5c	*Upper Evaporites*	*Upper Evaporites*	*Upper Evaporites*	UU (Upper Unit)	UU (Upper Unit)	UU (Upper Unit)	*Undifferentiated evaporites*
U5b	*Salt (Halite)*	*Messinian salt*	*Messinian salt*	MU (Mobile Unit)	MU (Mobile Unit)	MU (Mobile Unit)	*Undifferentiated evaporites*
U5a		*Lower Evaporites ? (upper part of U5a)*	*Lower Evaporites (upper part of U5a)*	LU (Lower Unit - upper part of U5a)	LU1	LU (Lower Unit - upper part of U5a)	*Undifferentiated evaporites*
U4c	*Messinian detritic deposits*	Detrital	Unit D	CU (Chaotic Unit)	Dm2	CU (Complex Unit)	c (*Messinian deposits*)
Base U4c (minor erosion)			*MES (Messinian Erosional Surface)*	*BES (Bottom Erosional surface)*		*BES (Bottom Erosional surface)*	
U4b	*Miocene*		*Miocene*	C1 to C5	Dm1-LU0	*Mio*	c (*Messinian deposits*)
U4a	*Miocene*		*Miocene*	C1 to C5	Dm0-LU0	*Mio*	c (*Messinian deposits*)
S3				ES1	Base Dm	*First Miocene submarine canyon*	b (*BES, Bottom Erosional Surface*)
U3	*Miocene*	*Miocene*		*Mio*	*Miocene shelf*	*Mio*	*a (Miocene shelf)*

Supplementary Figure 3. Comparison between the naming convention used in this study and published naming conventions.

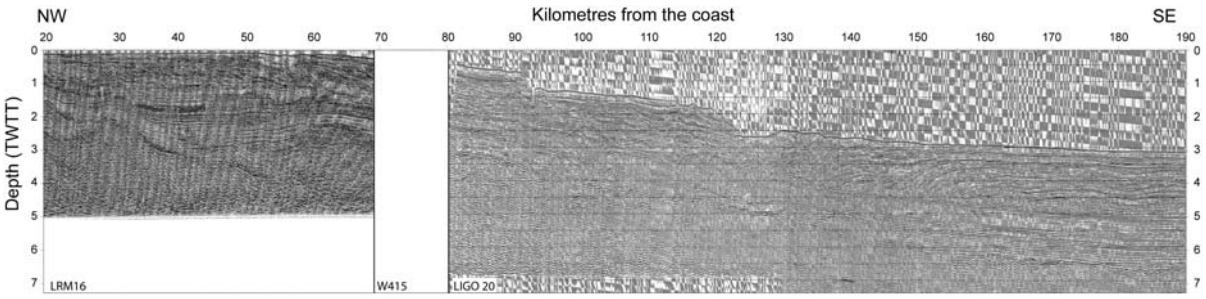

Supplementary Figure 4. Uninterpreted seismic profiles Ligo 20 and LRM 16 used for the line drawing of Fig. 3.

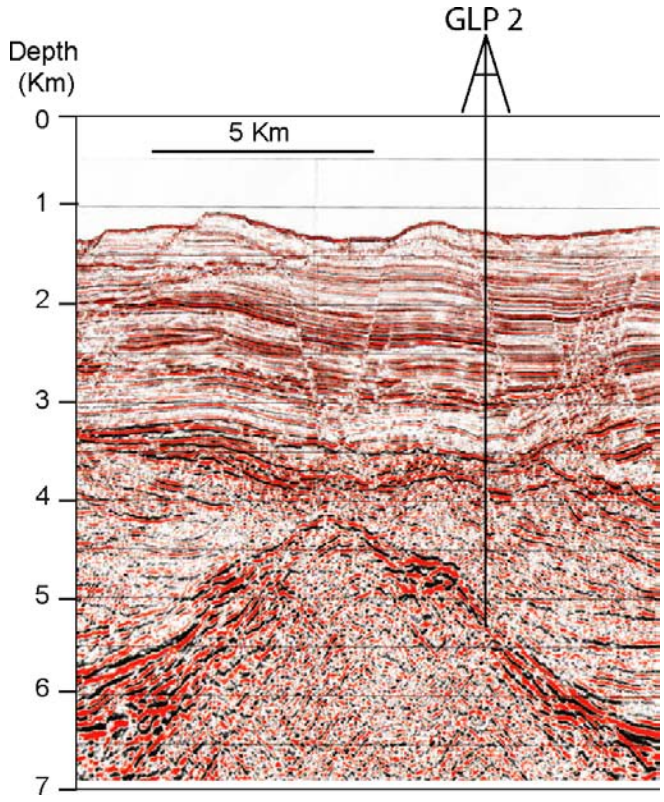

Supplementary Figure 5. Uninterpreted seismic profile of Fig. 11.

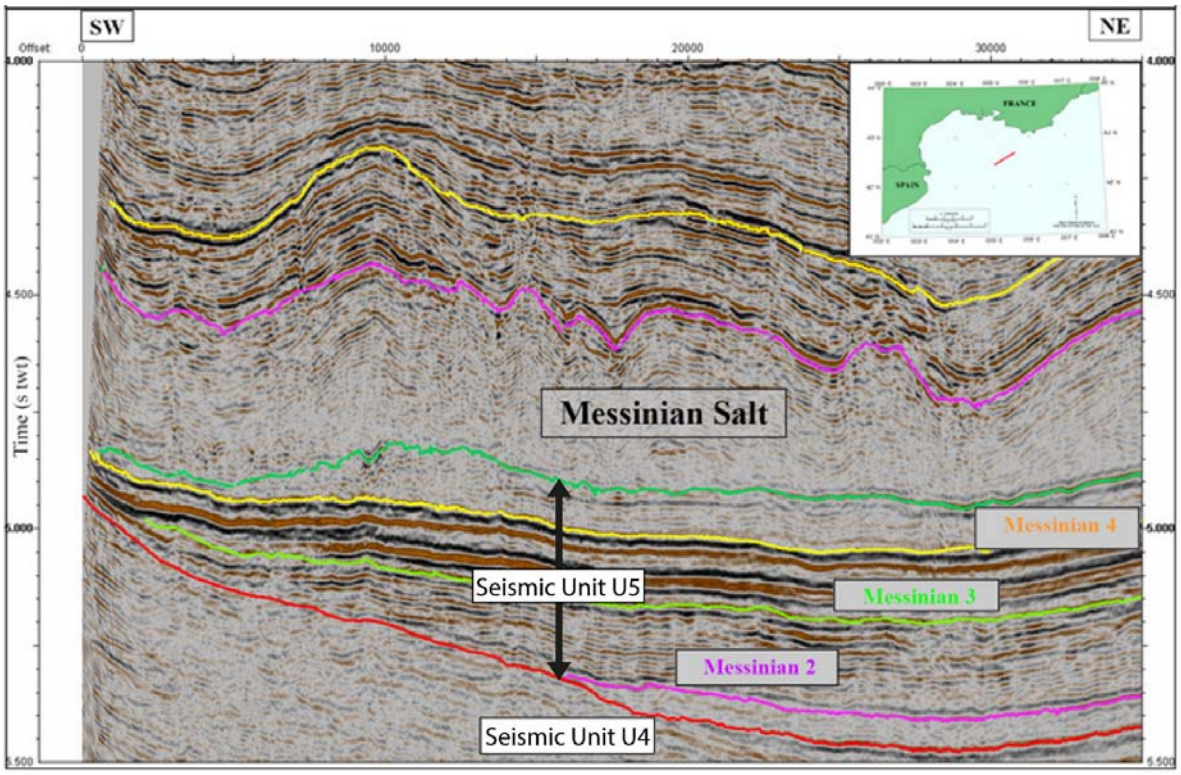

Supplementary Figure 6. Seismic profile in the Gulf of Lions showing onlap deposition of seismic unit U5 (which includes Messinian 2 to 4 on the figure) on seismic unit U4 (modified from Ianev et al. (2007)).